Nanomagnetism

Part 2 – Domains and domain walls

Olivier Fruchart

Institut Néel (Univ. Grenoble Alpes – CNRS)
Grenoble – France

http://neel.cnrs.fr

Micro-NanoMagnetism team : http://neel.cnrs.fr/mnm

Part 1 : basics of micromagnetism – Simple models of magnetization reversal

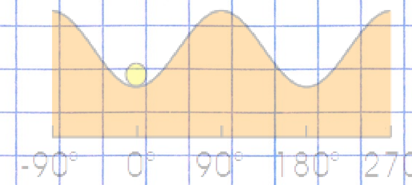

Part 2 : non-uniform magnetization in nanostructure: domains, domain walls

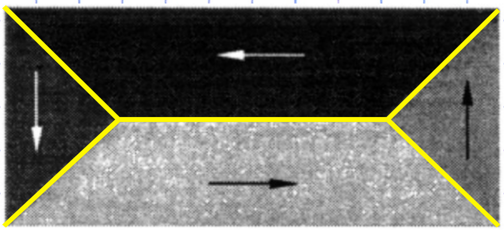

Part 3 : Low-dimensions, interfaces and heterostructures

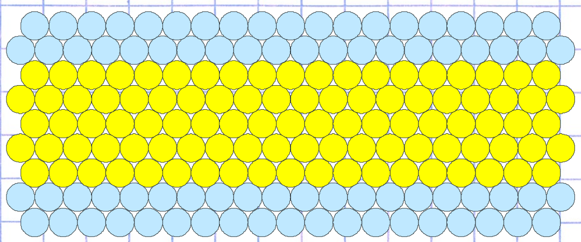

Part 4 : Learn from hysteresis loops

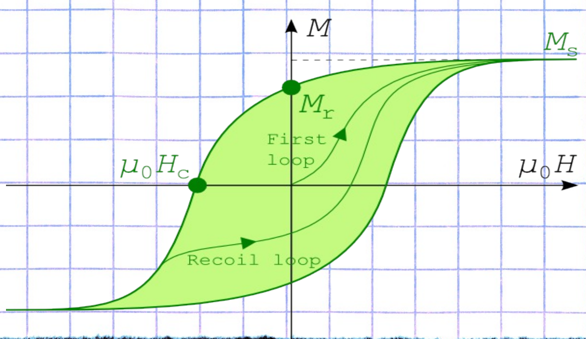

Theory, 'Astroid' curve

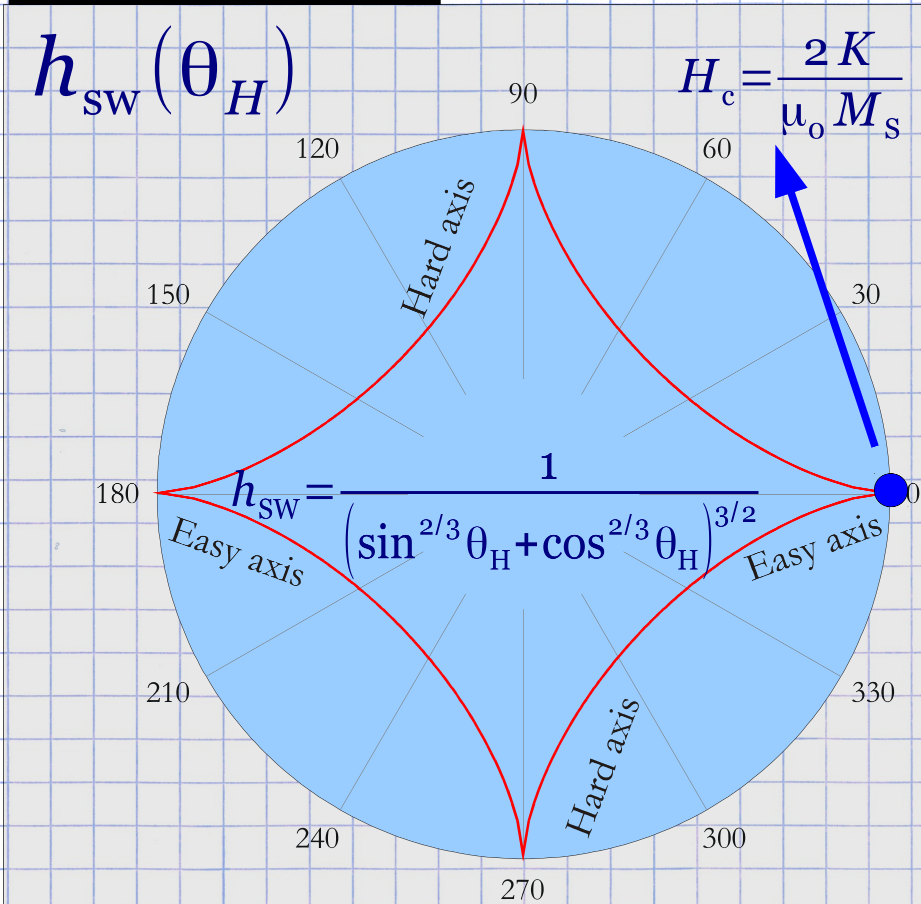

Experiments

$$H_c \ll \frac{2K}{\mu_0 M_s}$$

Known as Brown paradox

W. F. Brown, Jr., Micromagnetics (Wiley, New York, 1963)

Seeking understanding

- Non-uniform distributions of magnetization
- Origin may be intrinsic (eg shape) or extrinsic (defect)

Bulk material

Numerous and complex magnetic domains

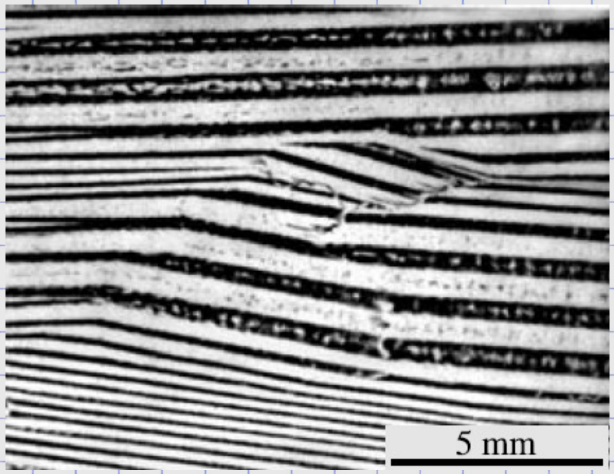

FeSi soft sheet

A. Hubert, *Magnetic domains*

Mesoscopic scale

Small number of domains, simple shape

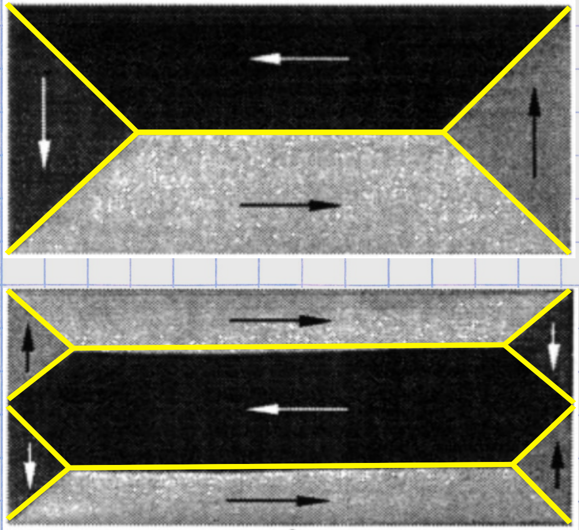

Microfabricated dots
Kerr magnetic imaging

A. Hubert, *Magnetic domains*

Nanometric scale

Magnetic single-domain

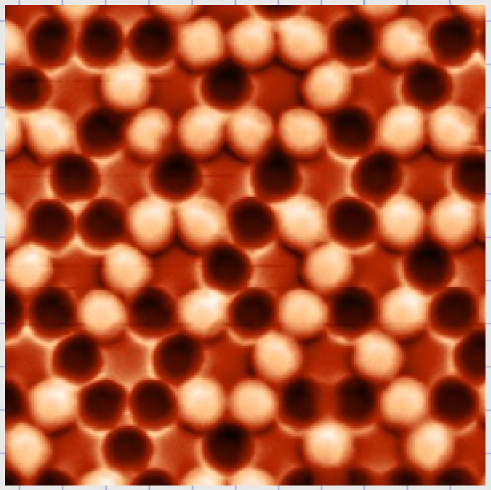

Nanofabricated dots
MFM

I. A. Chioar, PRB90, 064411 (2014)

- Domain walls play a crucial role in magnetization processes
- Domain walls define length scales

Anisotropy exchange length

$$E = A\left(\partial_x\theta\right)^2 + K_\mathrm{u}\sin^2\theta$$

Exchange → J/m

Anisotropy → J/m^3

Anisotropy exchange length $\Delta_\mathrm{u} = \sqrt{A/K_\mathrm{u}}$

$\Delta_\mathrm{u} \approx 1\ \mathrm{nm}$ → $\Delta_\mathrm{u} \geq 100\ \mathrm{nm}$

Hard — Soft

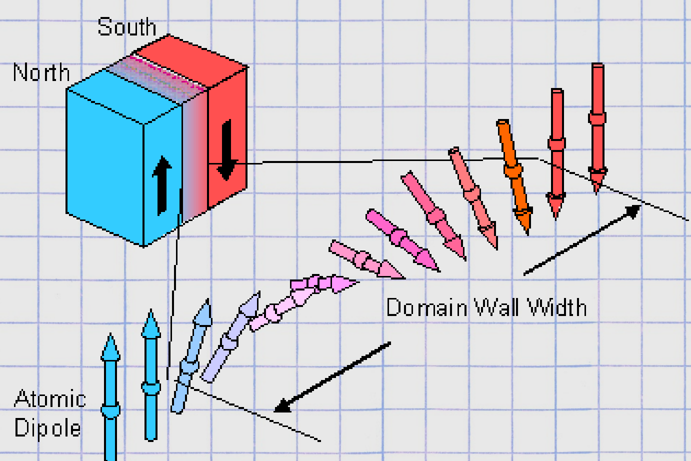

Often called *Bloch parameter* or *domain-wall width*

Dipolar exchange length

$$E = A\left(\partial_x\theta\right)^2 + K_\mathrm{d}\sin^2\theta$$

Exchange → J/m

Dipolar energy → J/m^3

$$K_\mathrm{d} = \frac{1}{2}\mu_0 M_\mathrm{s}^2$$

Dipolar exchange length:

$$\Delta_\mathrm{d} = \sqrt{A/K_\mathrm{d}}$$
$$= \sqrt{2A/\mu_0 M_\mathrm{s}^2}$$

$\Delta_\mathrm{d} \approx 3-10\ \mathrm{nm}$

Single-domain critical size relevant for nanoparticules made of soft magnetic material

Often called *Exchange length*

Notice:

Other length scales: with field etc.

Linear model

Naïve however provides all physics

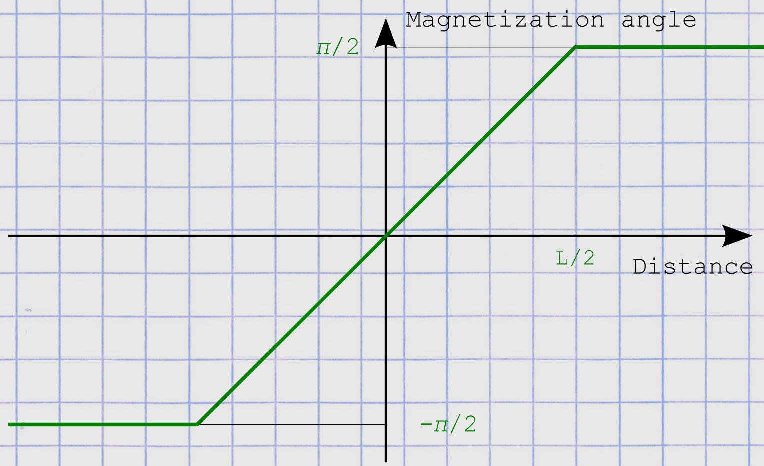

$$E_{ex}=A(\nabla.\mathbf{m})^2=A(\pi/L)^2$$

$$\langle E_u\rangle=K_u\langle\cos^2\theta\rangle=K_u/2$$

Feature of domain walls

	Linear	Exact
Width	$\Lambda_W=\pi\sqrt{2}\sqrt{A/K_u}$	$\Lambda_W=\pi\sqrt{A/K_u}$
Energy	$\mathcal{E}=\pi\sqrt{2}\sqrt{AK_u}$	$\mathcal{E}=4\sqrt{AK_u}$

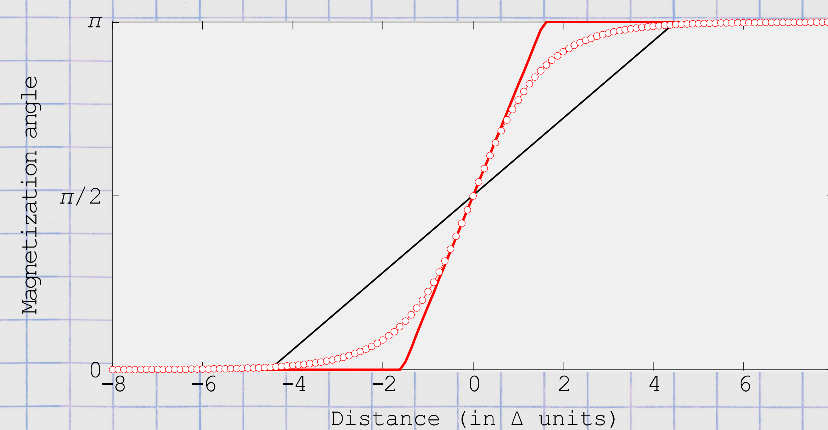

Domain walls and coercivity

- Soliton-like propagation : no deformation, requires no energy (NB : under quasistatic conditions)
- Contribution to coercivity requires geometrical or material inhomogenities

Brown's paradox

In most systems $H_c \ll \dfrac{2K}{\mu_0 M_s}$

Micromagnetic modeling

Exhibit analytic however realistic models for magnetization reversal

PHYSICAL REVIEW VOLUME 119, NUMBER 1 JULY 1, 1960

Reduction in Coercive Force Caused by a Certain Type of Imperfection

A. Aharoni
Department of Electronics, The Weizmann Institute of Science, Rehovot, Israel

(Received February 1, 1960)

As a first approach to the study of the dependence of the coercive force on imperfections in materials which have high magnetocrystalline anisotropy, the following one-dimensional model is treated. A material which is infinite in all directions has an infinite slab of finite width in which the anisotropy is 0. The coercive force is calculated as a function of the slab width. It is found that for relatively small widths there is a considerable reduction in the coercive force with respect to perfect material, but reduction saturates rapidly so that it is never by more than a factor of 4.

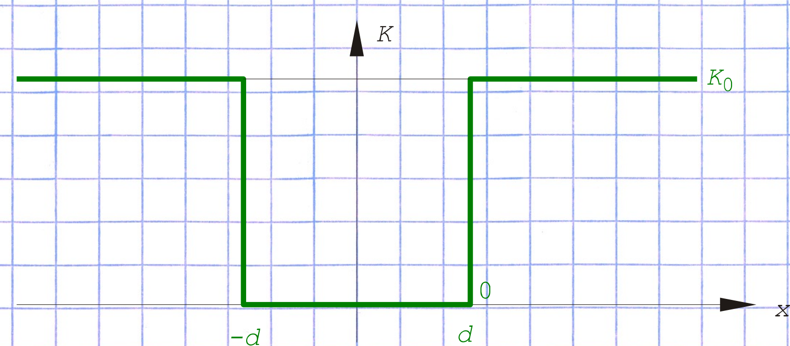

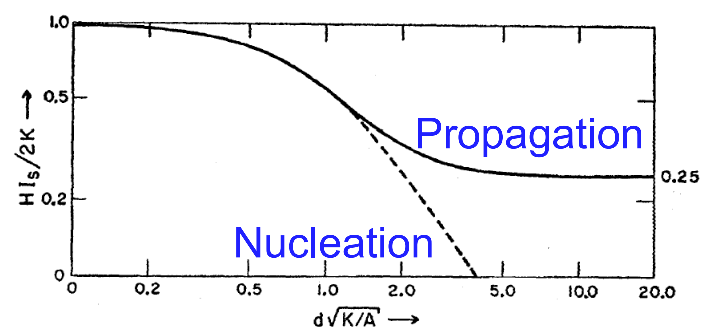

Fig. 1. The nucleation field (dashed) and coercive force (full curve) in terms of the coercive force of perfect material, $HI_s/2K$, as functions of the defect size, d.

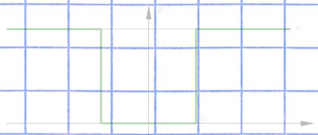
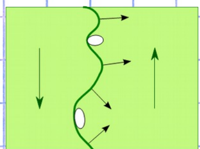
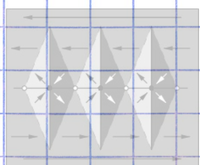
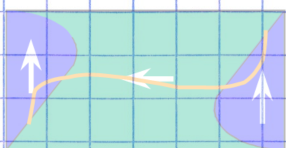
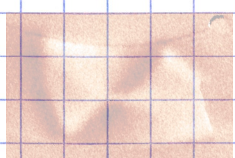
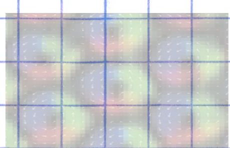

Coercivity determined by nucleation | **Coercivity determined by propagation**

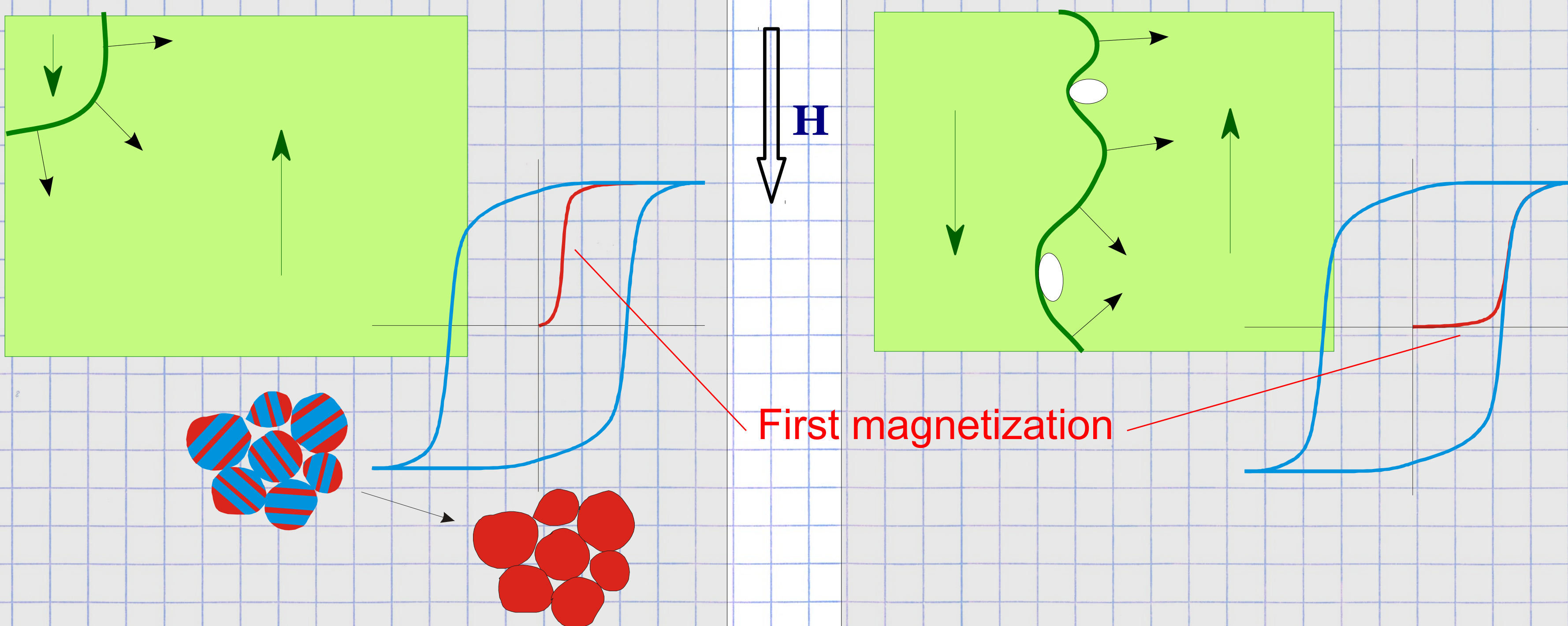

⇨ Physics has some similarity with that of grains

⇨ Concept of nucleation volume

⇨ Physics of surface/string in heterogeneous landscape

⇨ Modeling necessary

Activation volume

Also called: nucleation volume

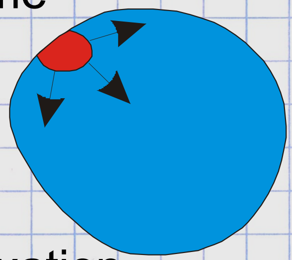

Can be used for:

- Estimating Hc(T)
- Estimating long-time relaxation
- Determination of dimensionality

Note: of the order of domain wall width δ

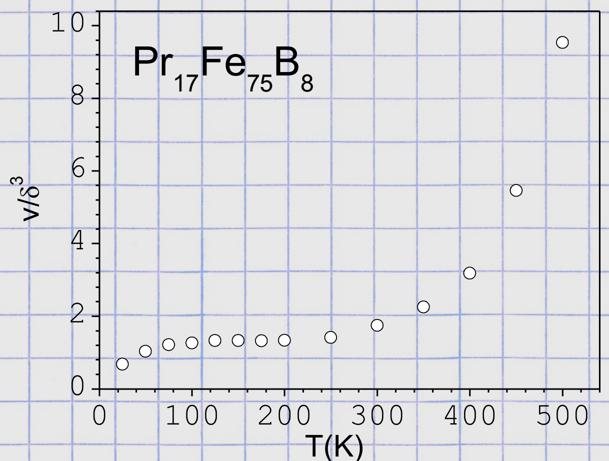

Courtesy D. Givord

More detailed models:

D. Givord et al., JMMM258, 1 (2003)

1/cosθ law

E. J. Kondorsky, J. Exp. Theor. Fiz. 10, 420 (1940)

Hypothesis:

- Based on nucleation volume
- Hc<<Ha

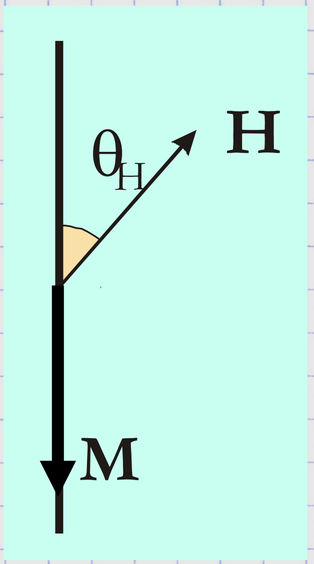

Energy barrier E_0 overcome by gain in Zeeman energy plus thermal energy

$$E_o = -\mu_o M_S v_a H \cos\theta_H + 25 k_B T$$

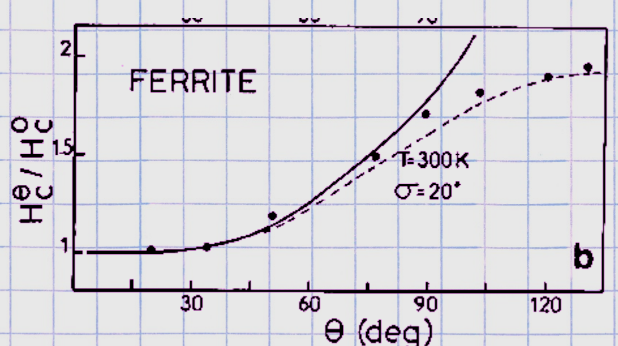

D. Givord et al., JMMM72, 247 (1988)

Nucleation of new reversed domains

Fatuzzo/Labrune/Raquet model

$$dN = (N_o - N) R \, dt$$

$$\Rightarrow N = N_o [1 - \exp(-Rt)]$$

N: number of nucleated centers at time *t*

N_0: total number of possible nucleation centers

R: rate of nucleation

Radial expansion of existing domains

$$\sigma_n = \sigma - \sigma_c = (v_0^2/T)[t_0 + t]^2 - \pi r_c^2 / T$$

$$A = \underbrace{\int_0^t \left(\frac{dN}{dt}\right)_s (\sigma_n)_{t-s} ds}_{\text{Growth of existing nuclei}} + \underbrace{\frac{\pi r_c^2}{T} N(t)}_{\text{New nuclei}}$$

r_c: radius of critical nucleus

T: total area of sample

V_0: speed of propagation of domain wall

Combination → Predicts area not yet reversed

$$\Rightarrow B(t) = \exp\Big(-2k^2\Big(1 - (Rt + k^{-1}) + \tfrac{1}{2}(Rt + k^{-1})^2 - e^{-Rt}(1 - k^{-1}) - \tfrac{1}{2}k^{-2}(1 - Rt)\Big)\Big),$$

$$k = v_o / (R r_c)$$

k is a measure of the importance of wall propagation versus nucleation events

E. Fatuzzo, Phys. Rev. 127, 1999 (1962)

Depending on structural defects

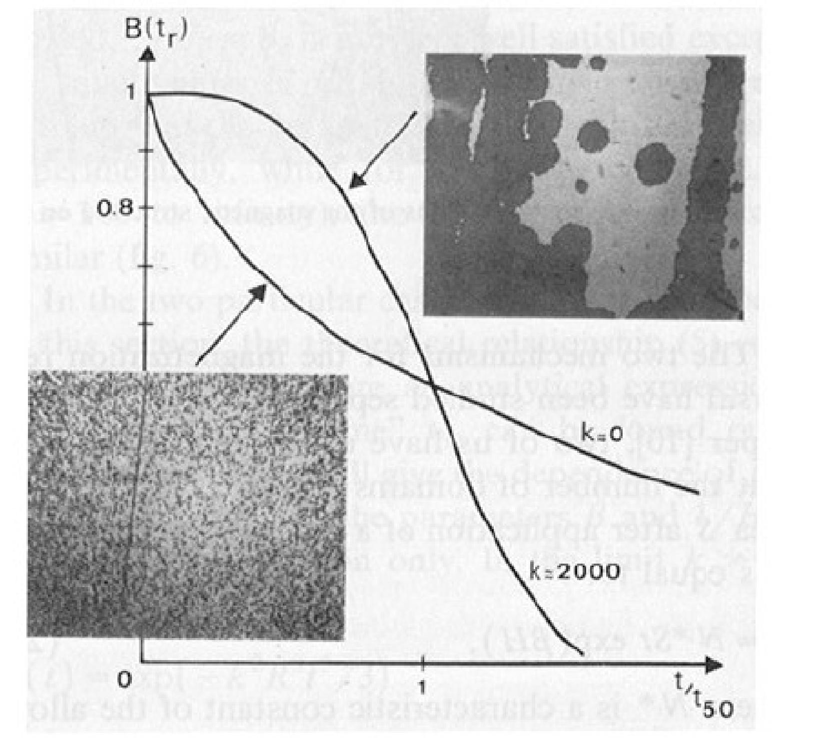

Fig. 4. Magnetization versus reduced time t_R for a GdFe sample ($k \approx 2000$) and a TbCo one ($k \approx 0$), corresponding domain structure observed by Kerr effect.

M. Labrune et al., J. Magn. Magn. Mater. 80, 211 (1989)

Depending on measurement dynamics

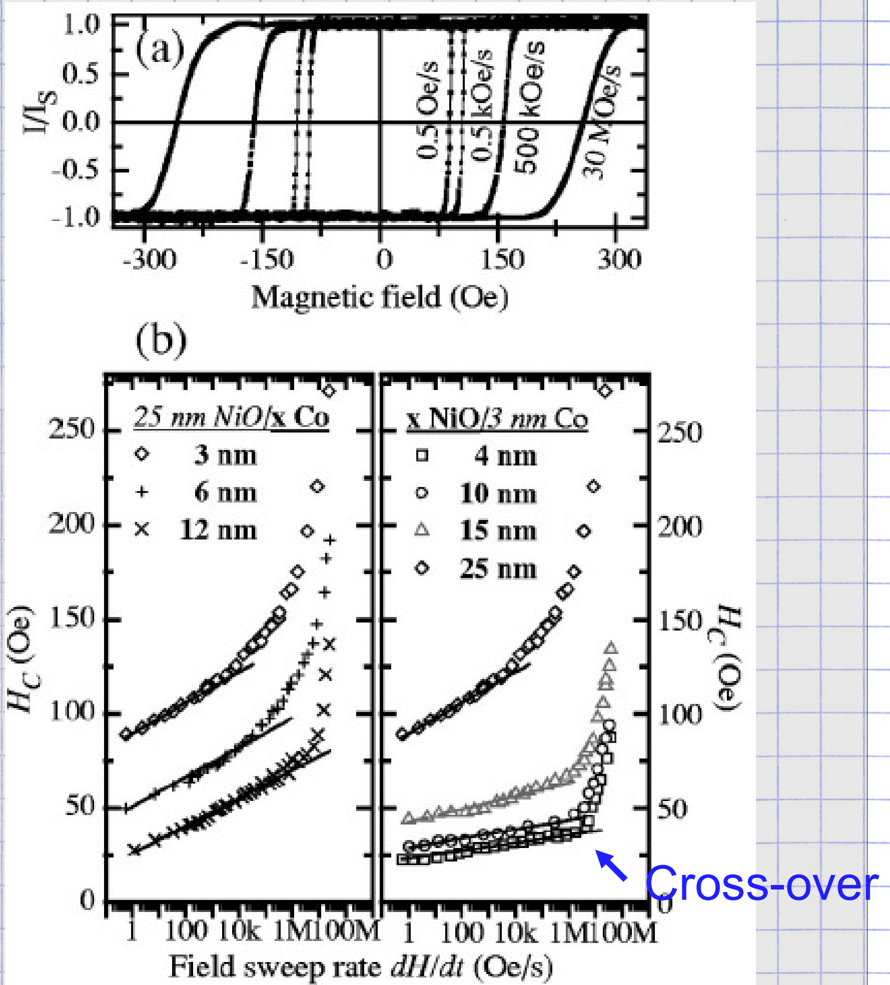

J. Camarero et al., PRB64, 172402 (2001)

Note also for fast propagation of domain walls: breakdown of propagation speed (Walker)

Theory

⇨ Physics : rope in a 2D medium with static disorder

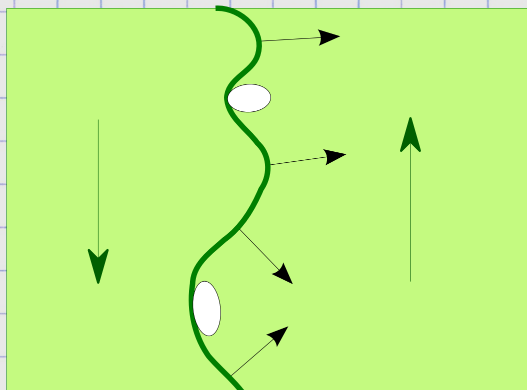

⇨ Energy barriers scale like $(1/H)^{\mu}$

⇨ Domain wall speed determined by Arrhenius law

$$v(H) \sim \exp\left[-\beta U_c \left(\frac{H_{crit}}{H}\right)^{\mu}\right]$$

S. Lemerle et al., PRB80, 849 (1998)

Experiment

Pt/Co/Pt film, perpendicular anisotropy

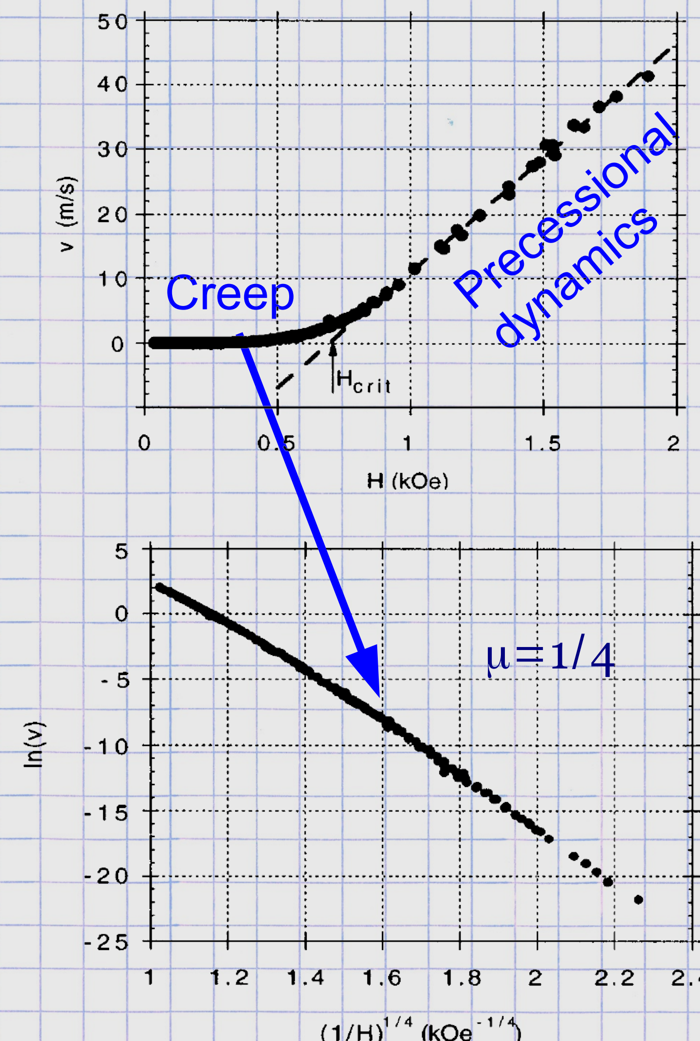

Bloch versus Néel wall

Crude model: wall is a uniformly-magnetized cylinder with an ellipsoid base

Bloch wall

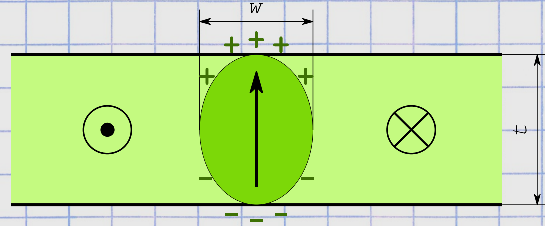

$$E_d \approx K_d \frac{W}{2t}$$

Thickness t

Wall width W

Néel wall

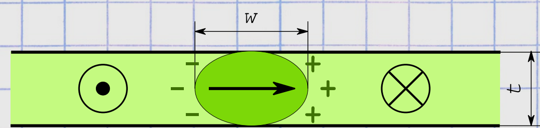

$$E_d \approx K_d \frac{t}{2W}$$

L. Néel, Énergie des parois de Bloch dans les couches minces, C. R. Acad. Sci. 241, 533-536 (1955)

Take-away meessages

- At low thickness (roughly $t \approx W$) Bloch domain walls are expected to turn their magnetization in-plane > Néel wall
- Model needs to be refined
- Domain walls not changed for films with perpendicular magnetization

Néel caps occur atop Bloch walls to reduce surface and volume magnetic charges

$$\mathbf{M}.\mathbf{n}=0$$

$$-\mathrm{div}\,\mathbf{M}=-\frac{\partial M_x}{\partial x}-\frac{\partial M_y}{\partial y}-\frac{\partial M_z}{\partial z}$$

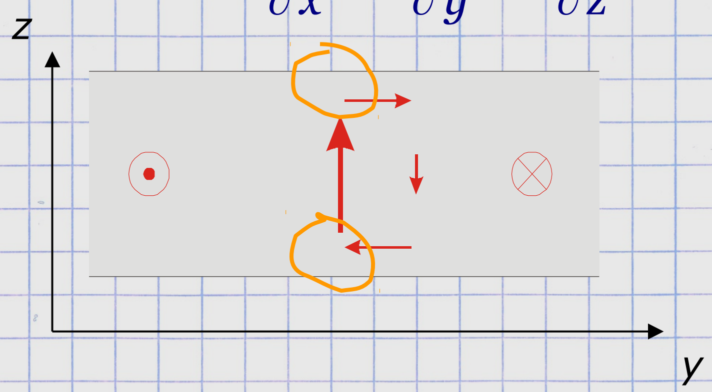

Refined phase diagram of domain walls

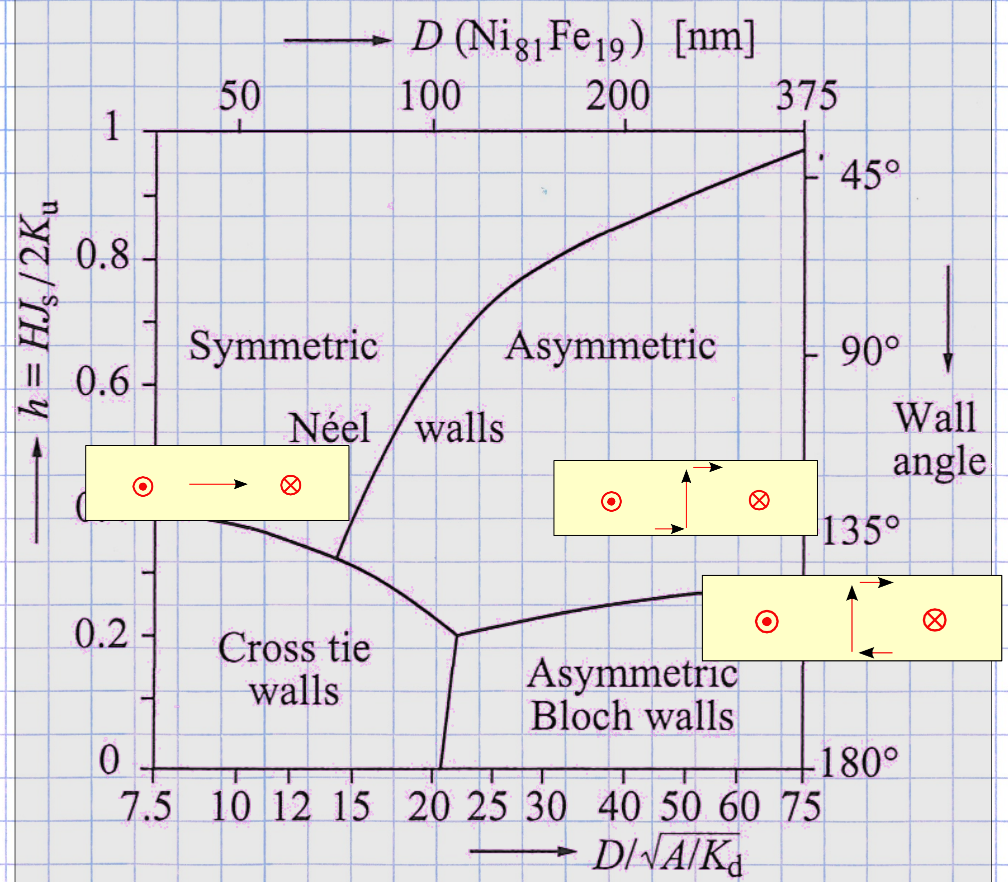

A. Hubert and R. Schäfer, Magnetic domains, Springer (1999)

From Néel walls to cross-tie walls

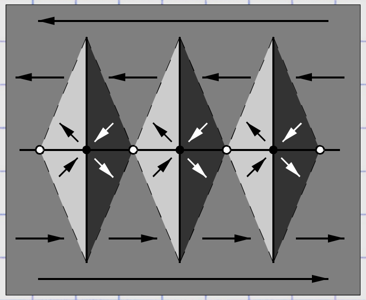

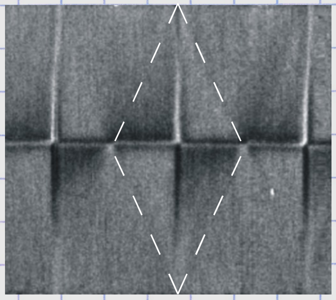

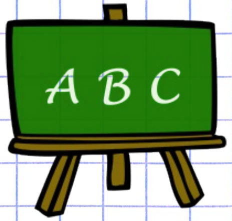

Domain pattern in asymmetric donut ?

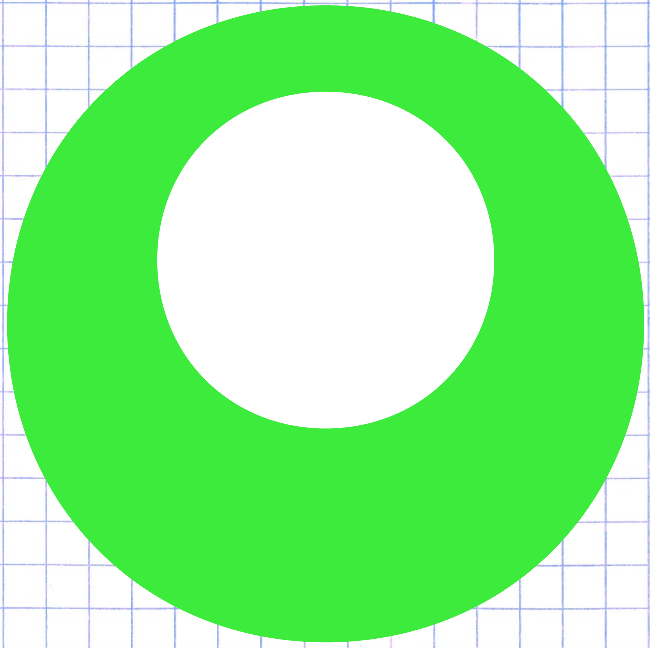

Hypothesis

Van den Berg model

Infinitely soft material $\mathcal{E}_{\mathrm{mc}}=0$

2D geometry (neglect thickness)

Zero external magnetic field $\mathcal{E}_{\mathrm{Z}}=0$

Size >> all magnetic length scales (wall width)

$\mathcal{E}_{\mathrm{ex}}\to 0$

Solution

Looking for a solution with : $\mathcal{E}_{\mathrm{d}}=0$

$-\operatorname{div}\mathbf{M}=0$ (no volume charges)

$\mathbf{M}.\mathbf{n}=0$ (no surface charges)

« Flux closure »

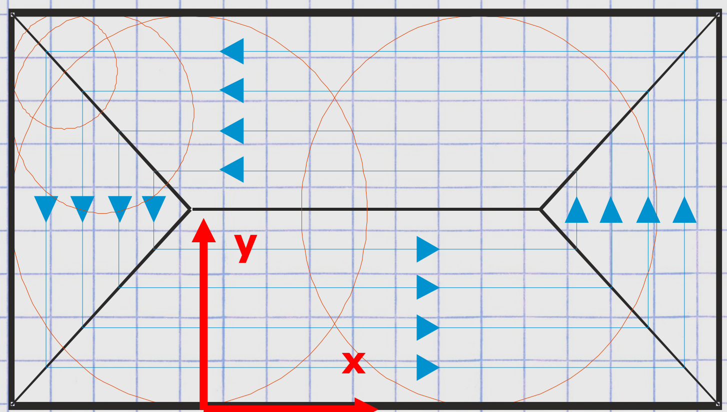

$$\operatorname{div}\mathbf{M}=\frac{\partial M_x}{\partial x}+\frac{\partial M_y}{\partial y}$$

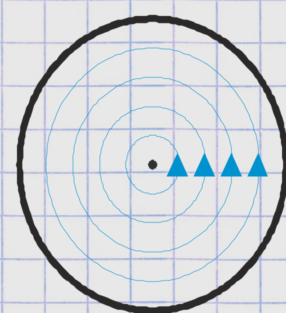

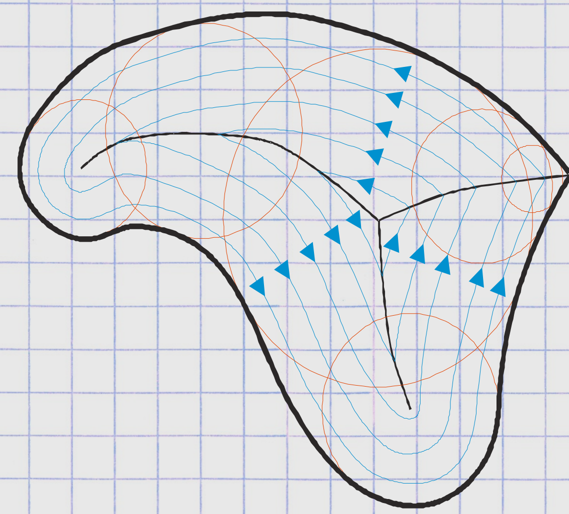

H. A. M. Van den Berg, *J. Magn. Magn. Mater.* 44, 207 (1984)

Sandpiles for simulating flux-closure patterns

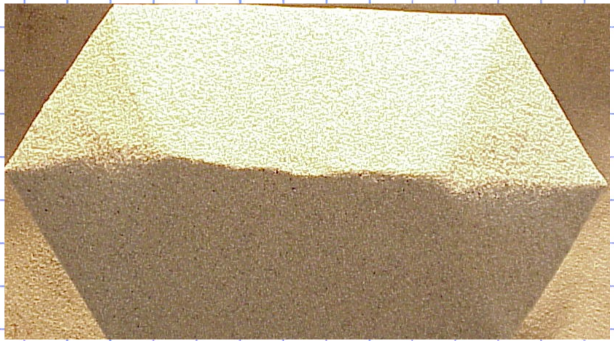

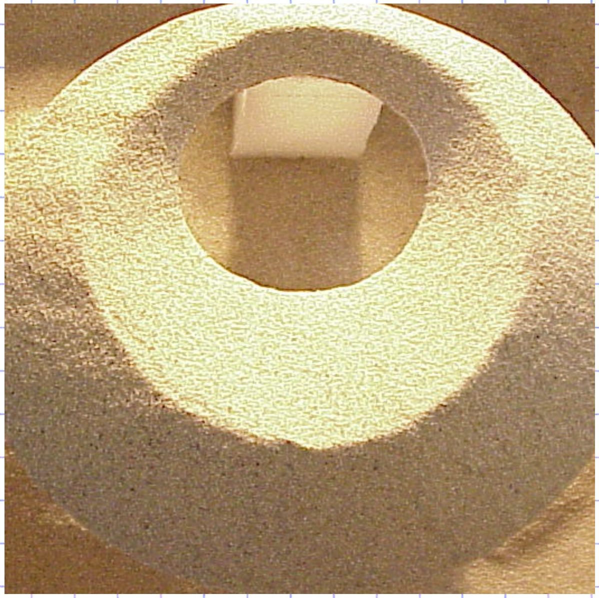

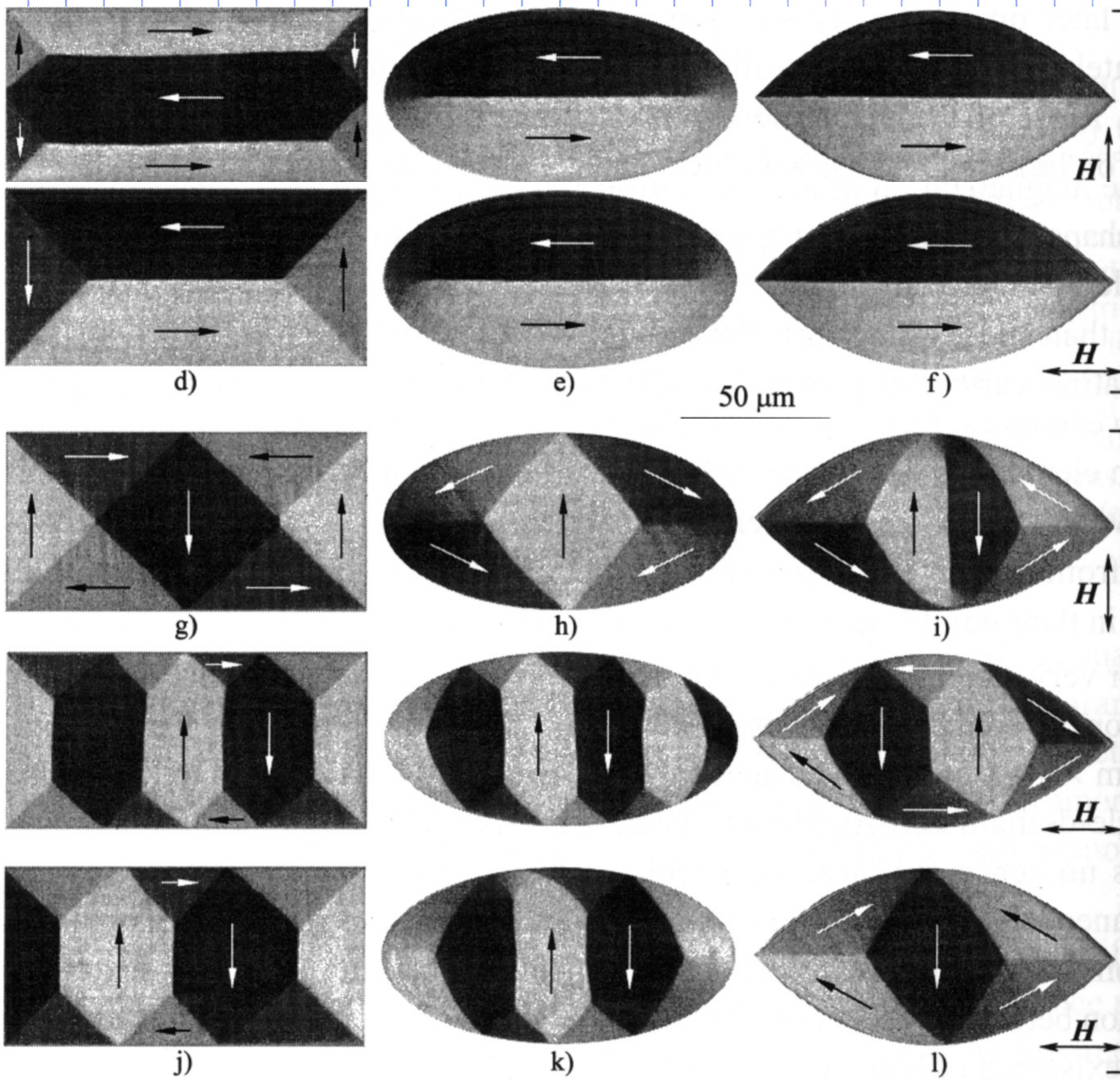

A. Hubert, *Magnetic domains*

Easy axis of **weak** magnetocrystalline anisotropy

Easy axis of **weak** magnetocrystalline anisotropy

Large dots

- many degres of freedom
- many possible states
- history is important
- even slight perturbations can influence the dot (anisotropy, defects, etc.).

Microscopic contribution to perpendicular anisotropy

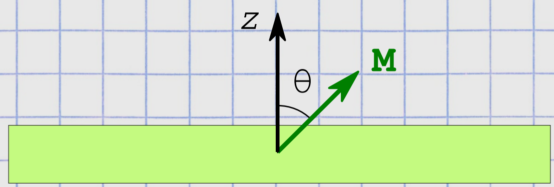

$E_{mc} = K_u \sin^2\theta$ $\quad K_u > 0$

⇨ Quality factor quantifies competition between miroscopic and dipolar energies

$$Q = \frac{K_u}{K_d}$$

$Q<1$

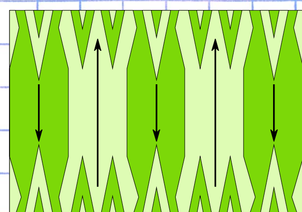

Branching

$W \sim t^{2/3}$

$t \gg t_c$

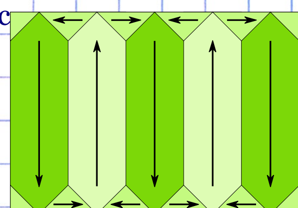

Strong stripe domains

$W \sim t^{1/2}$

$Q>1$

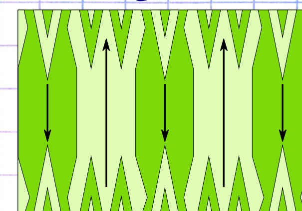

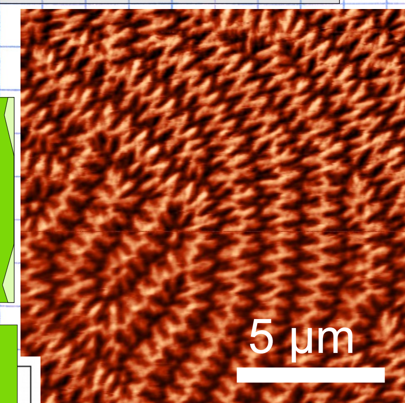

Semi-soft NdFeB

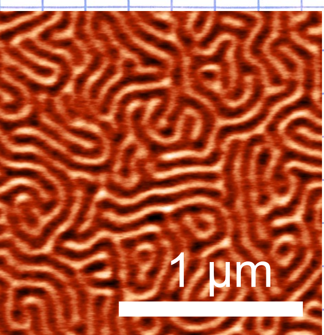

Ge3Mn5C

$t > t_c$ Weak stripe domains

$t_c = 2\pi\Delta_u$ Second-order transition

$t < t_c$ In-plane magnetized

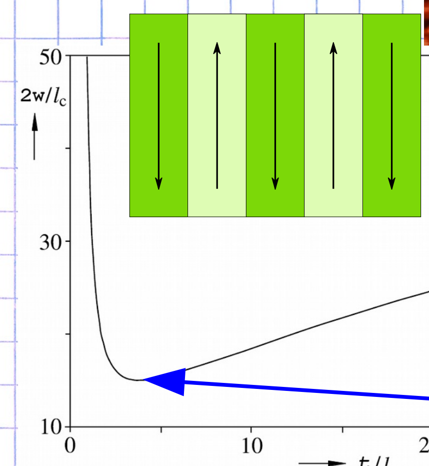

$$t_c \approx \frac{15Q}{2}\Delta_u$$

C. Kittel, Rev. Mod. Phys. 21 (4), 541 (1949)
Y. Murayama, J. Jap. Phys. Soc. 21, 2253 (1966)

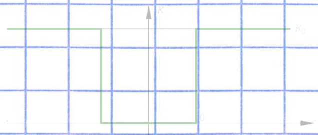

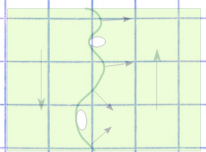

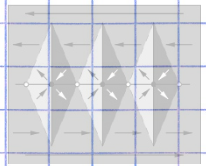

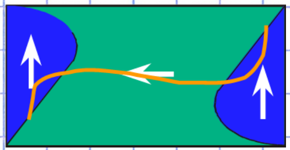

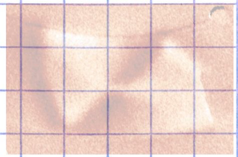

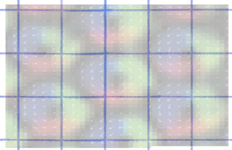

Experiments

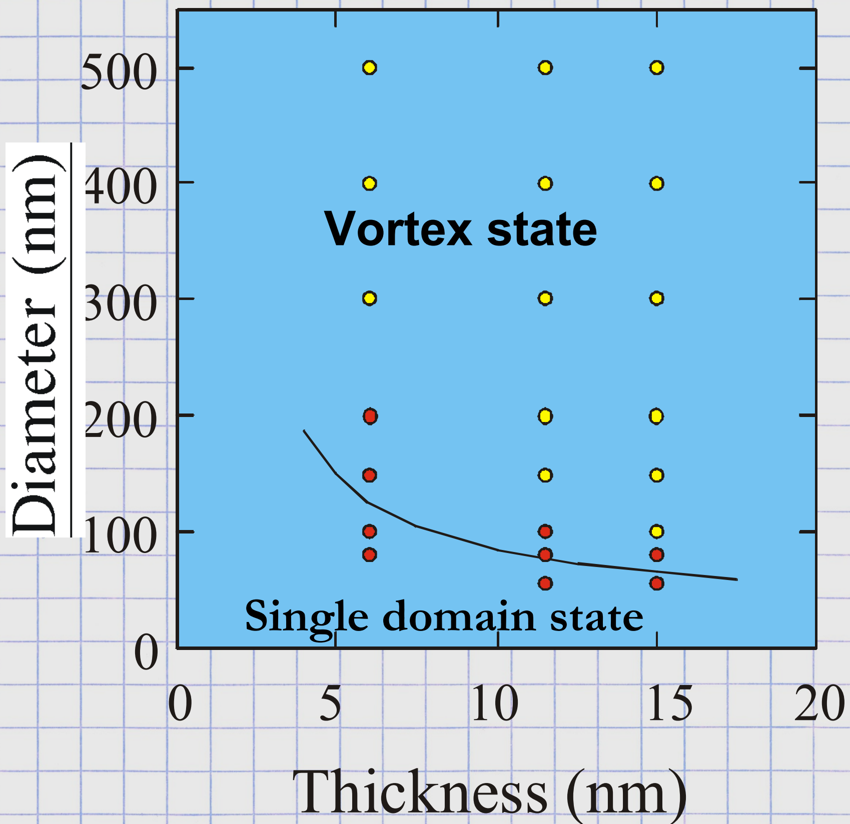

R.P. Cowburn, J.Phys.D:Appl.Phys.33, R1–R16 (2000)

Theory / Simulation

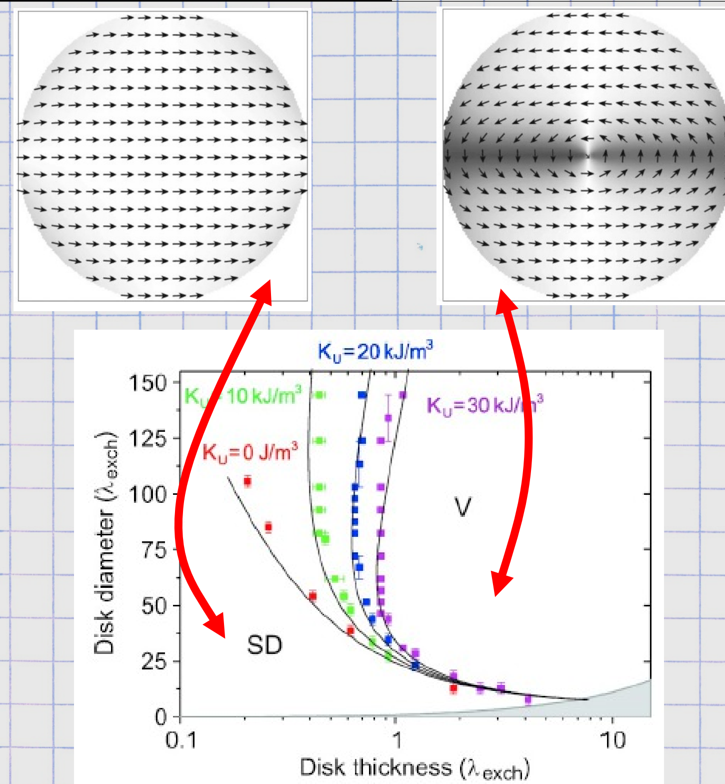

P.-O. Jubert & R. Allenspach, PRB 70, 144402/1-5 (2004)

Zero-field cross-over $t\,D \approx 20\,\Delta_d^2$

A B C

- Vortex state (flux-closure) dominates at large thickness and/or diameter
- The size limit for single-domain is much larger than the exchange length
- Experimentally the vortex may be difficult to reach close to the transition (hysteresis)

Experiments

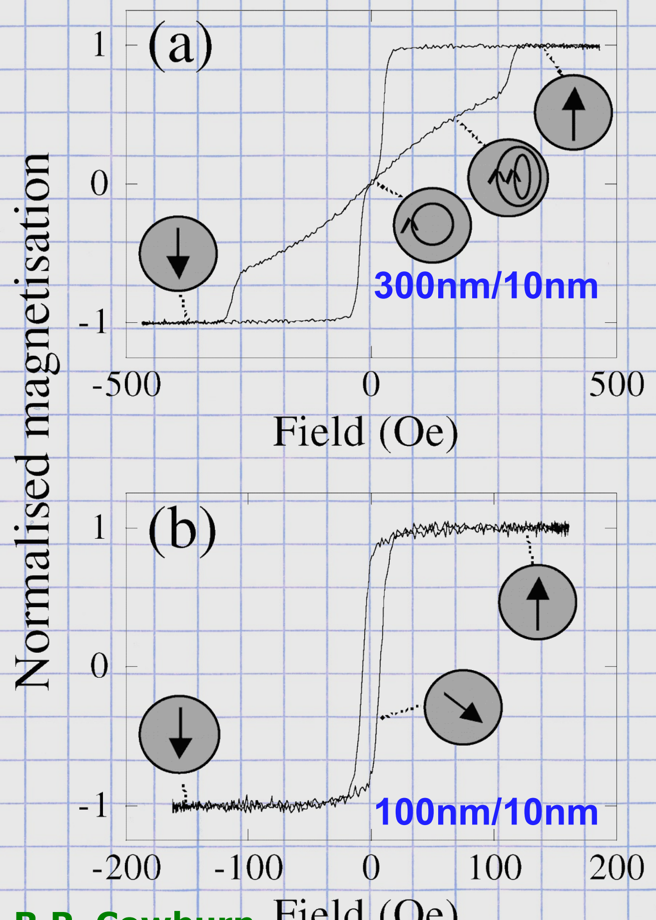

R.P. Cowburn, J.Phys.D:Appl.Phys.33, R1–R16 (2000)

Theory / Simulations

Displaced vortex model

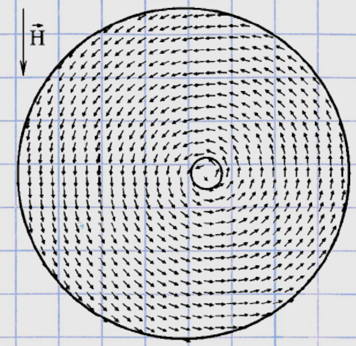

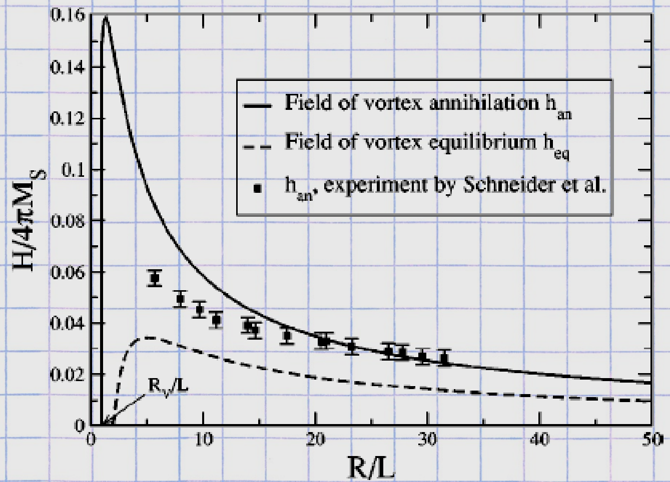

Calculation of the equilibrium line and the annihilation line

K. Y. Guslienko & K. L. Metlov, PRB 63, 100403(R) (2001)

- Typical loops for flux-closure states
- Energy of the vortex state can be computed from the anhysteretic above-loop area.

Upper bound for dipolar fields in 2D

Estimation of an upper range of dipolar field in a 2D system

$$\left\|\mathbf{H}_{\mathrm{d}}(R)\right\| \leqslant \int_{0}^{R} \frac{2\pi r}{r^3}\,\mathrm{d}r$$

Integration

Local dipole $1/r^3$

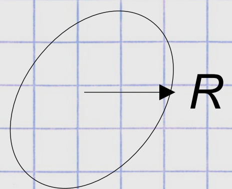

$$\left\|\mathbf{H}_{\mathrm{d}}(R)\right\| \leqslant \mathrm{Cte} + 1/R$$

Convergence with finite radius (typically thickness)

Non-homogeneity of dipolar fields in 2D

Example: flat strip with thickness/height = 0.0125

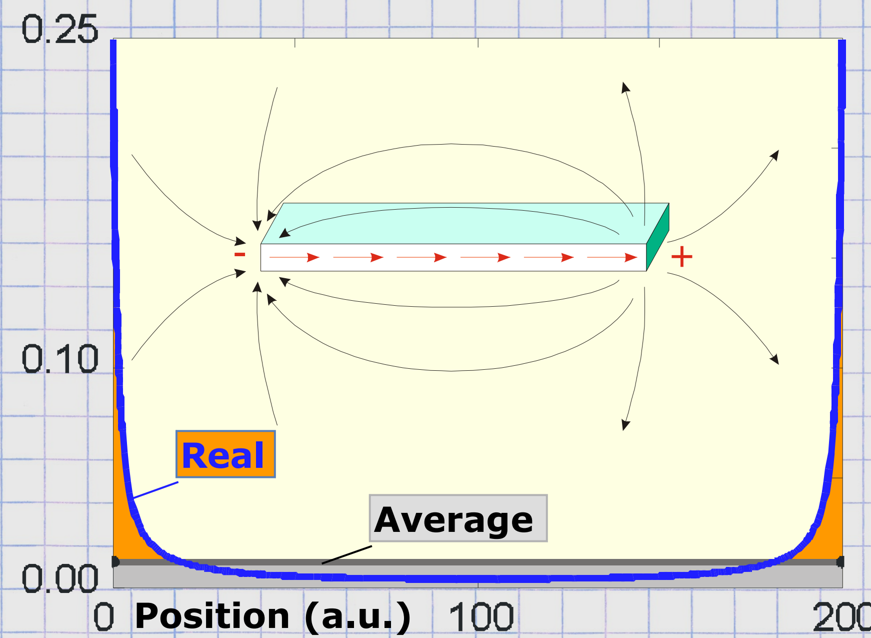

- Dipolar fields are weak and short-ranged in 2D or even lower-dimensionality systems
- Dipolar fields can be highly non-homogeneous in anisotropic systems like 2D
- Consequences on dot's non-homogenous state, magnetization reversal, collective effects etc.

Configurational anisotropy: deviations from single-domain

Strictly speaking, 'shape anisotropy' is of second order:

$$E_d = \frac{1}{2}\mu_0\left(N_x M_x^2 + N_y M_y^2 + N_z M_z^2\right)$$

2D: $\mathcal{E}_d = V K_d(\Delta N)\sin^2\theta$

In real samples magnetization is never perfectly uniform: competition between exchange and dipolar

Num.Calc. (100nm)

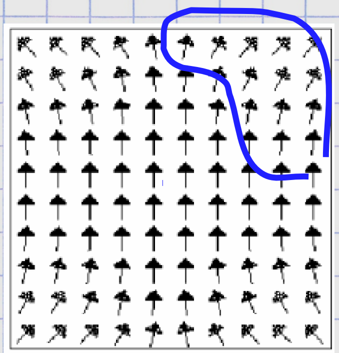

Flower state

$c/a > 2.7$

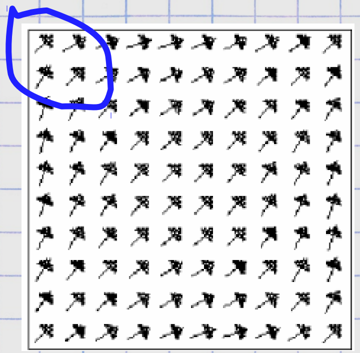

Leaf state

$c/a < 2.7$

Configurational anisotropy may be used to stabilize configurations against switching

⇨ Higher-order contributions to magnetic anisotropy

M. A. Schabes et al., JAP 64, 1347 (1988)

R.P. Cowburn et al., APL 72, 2041 (1998)

Polar plot of experimental configurational anisotropy with various symmetry

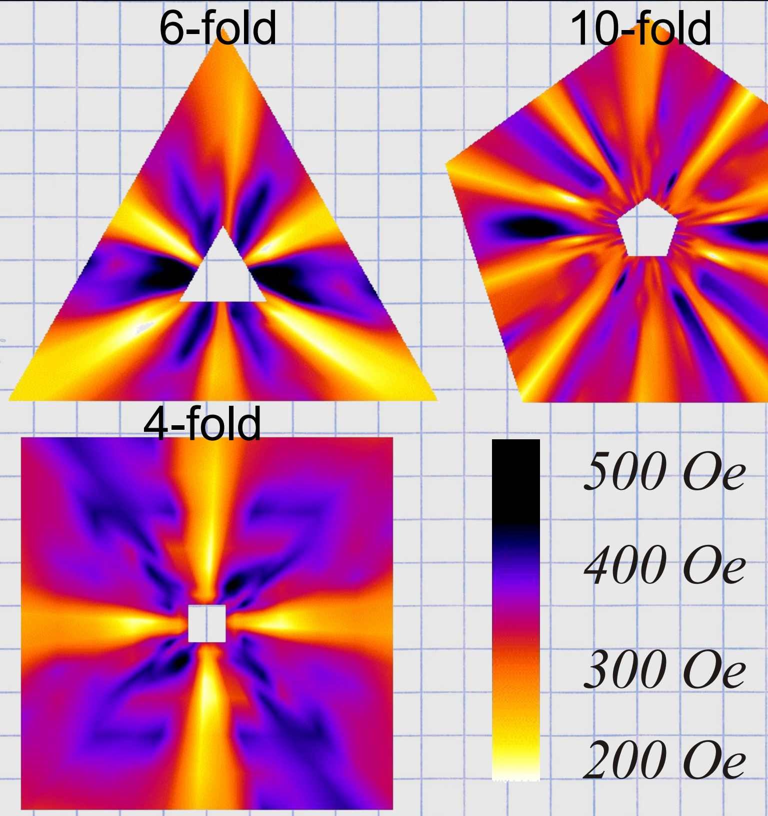

Color code: strength of anisotropy in a given direction

Radius: size of measured pattern

Direction: direction of measurement

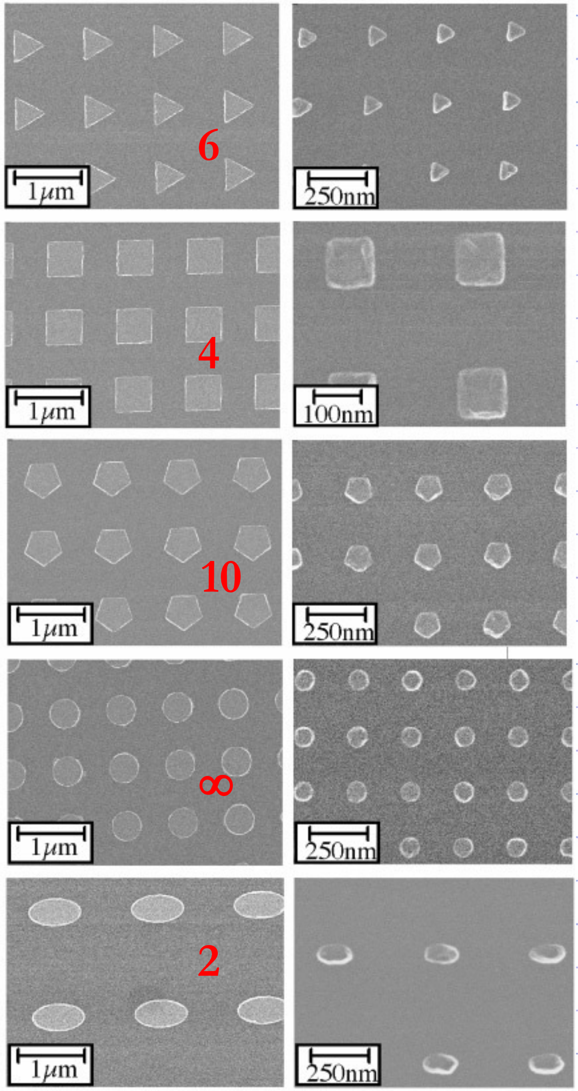

R.P. Cowburn, J.Phys.D:Appl.Phys.33, R1–R16 (2000)

'C' state

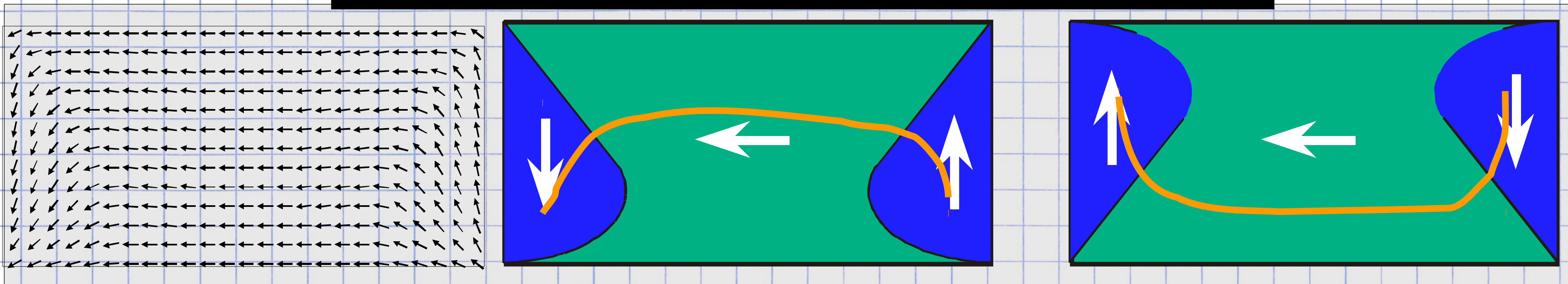

'S' state

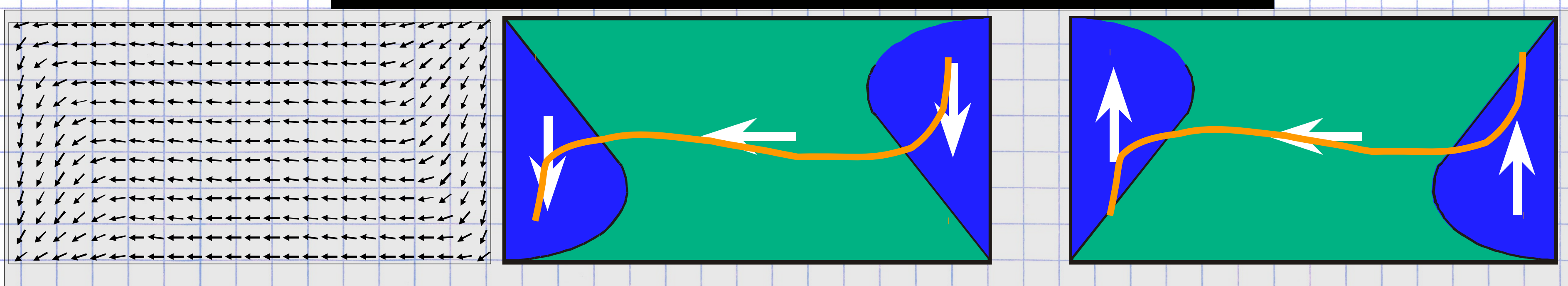

- At least 8 nearly-equivalent ground-states for a rectangular dot
- Issue for the reproductibility of magnetization reversal

Hypotheses ⇨ Soft magnetic material

⇨ Not too small neither too large nanostructures

Hc ~1/Width

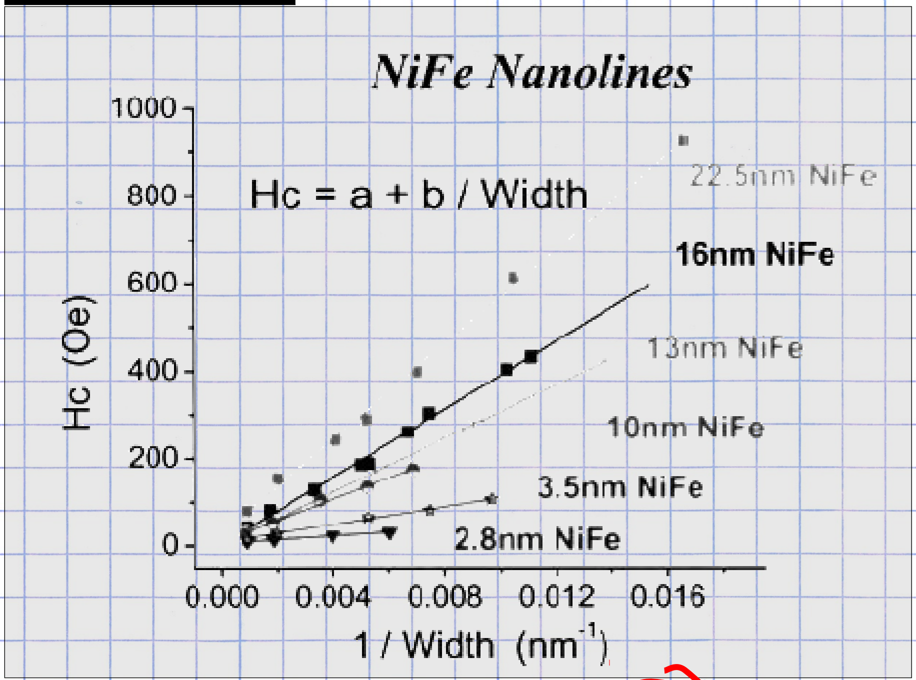

Hc ~Ms * Thickness

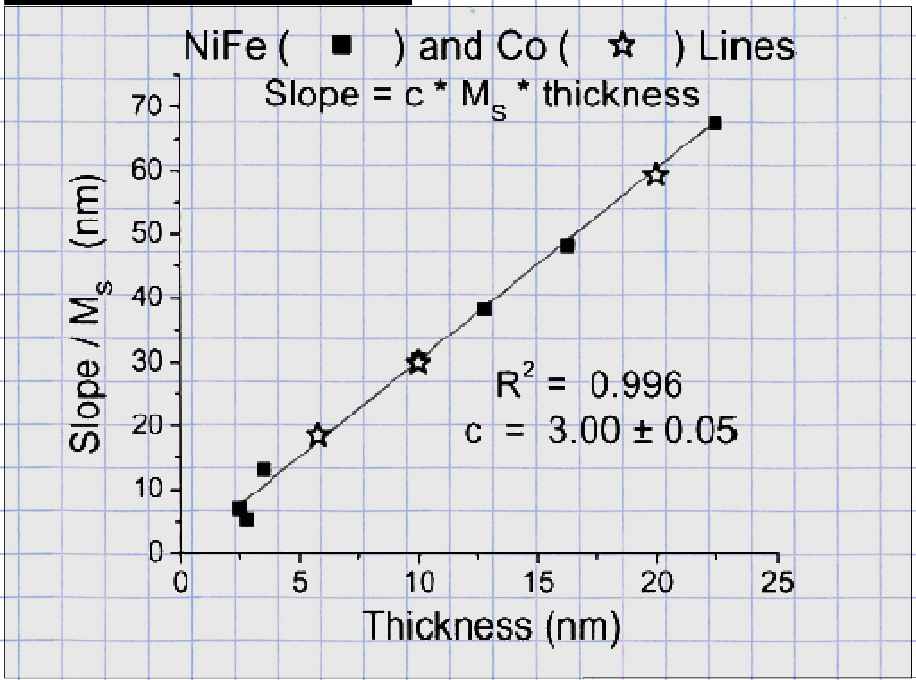

$$H_c \approx a + 3M_s \frac{t}{W}$$

~Lateral demagnetizing coefficient of the strip

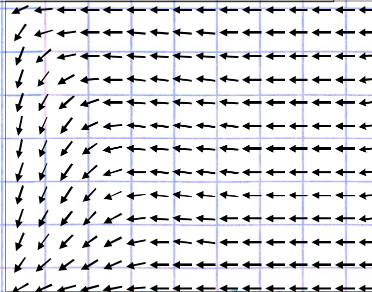

W. C. Uhlig & J. Shi,
Appl. Phys. Lett. 84, 759 (2004)

Magnetization is pinned at sharp ends

Experiments **Permalloy** (soft)

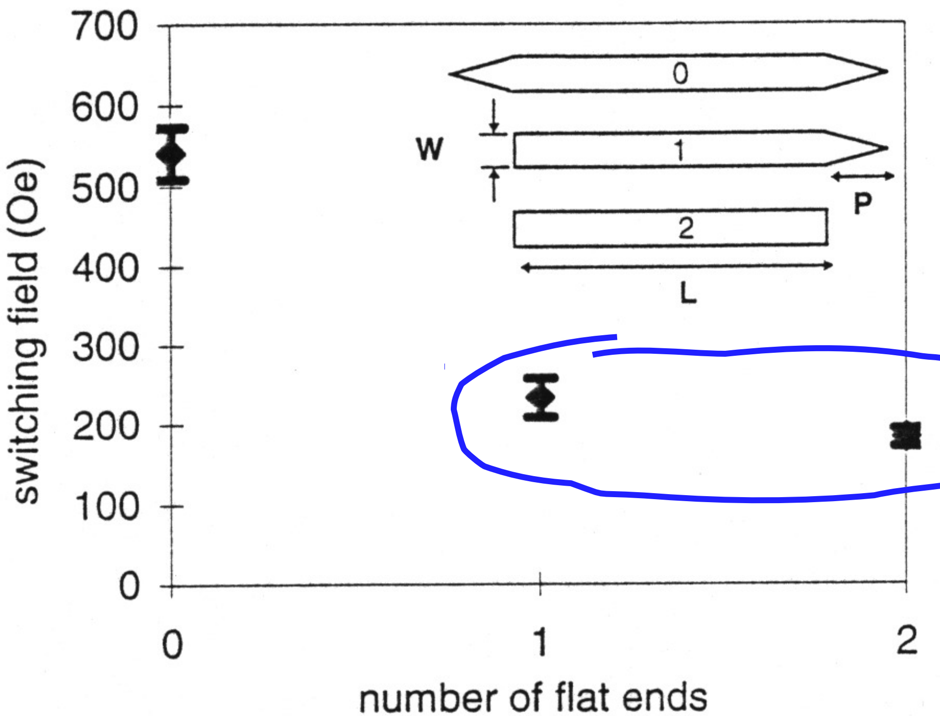

Similar

Fig. 8 Dependence of switching field of acicular elements on the number of flat ends. Element geometry is also shown: L = 2.5 μm, W = 200 nm, P = 500 nm.

K.J. Kirk et al., J. Magn. Soc. Jap., 21 (7), (1997) Towards superparamagnetism

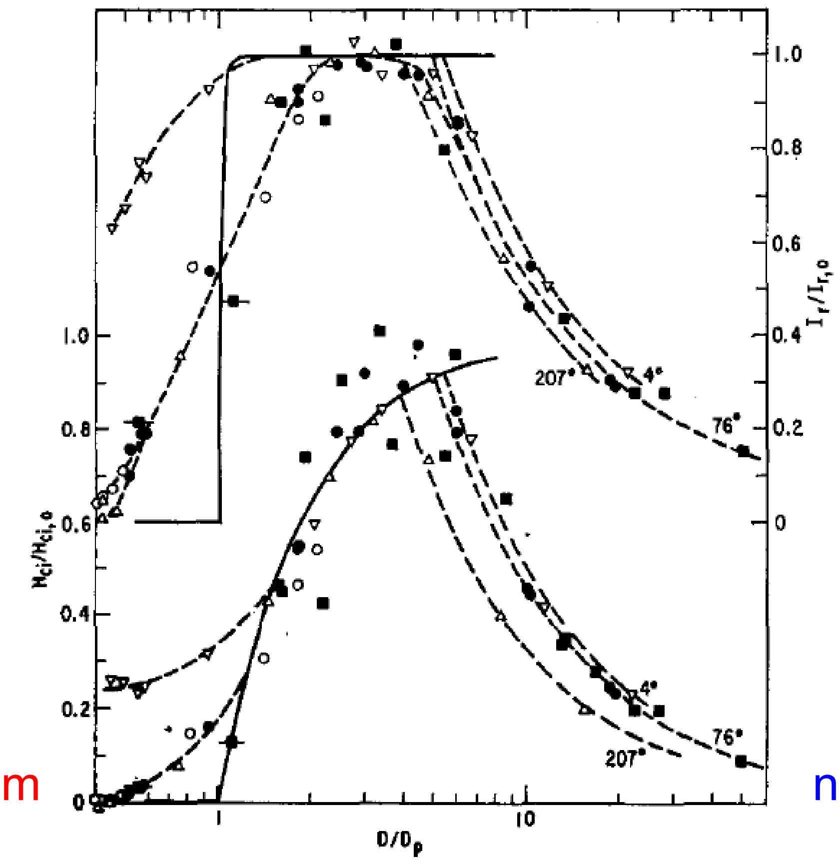

FIG. 1. Particle size dependence of essentially spherical, randomly oriented, iron particles. Calculated curve given by solid line. Diameters $D=\hat{d}_v$. Data at 76°K obtained from electron microscopic examination ■, calculated from I_r/I_s vs temperature O, and from smoothed data of H_{ci} vs D ●.

Towards nucleation-propagation and multidomain

E. F. Kneller & F. E. Luborsky,
Particle size dependence of coercivity and remanence of single-domain particles,
J. Appl. Phys. 34, 656 (1963)

Archetype for ferro coupling

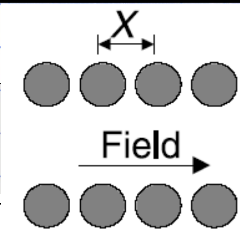

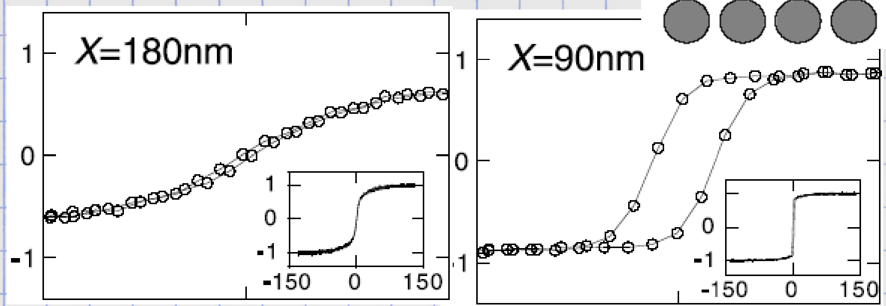

R. P. Cowburn et al., New J. Phys. 1, 1-9 (1999)

Archetype for AF coupling

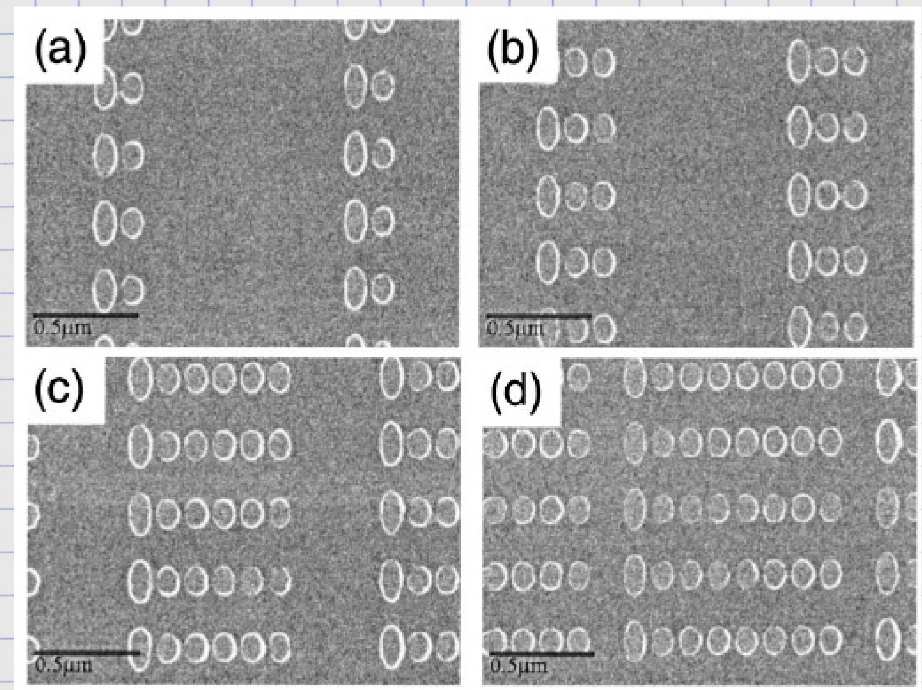

R. P. Cowburn, PRB65, 092409 (2002)

Conclusion:

Interactions increase energy barriers, with F or AF interactions

Cellular automata

Alternative to strips and domain walls to convey and process information

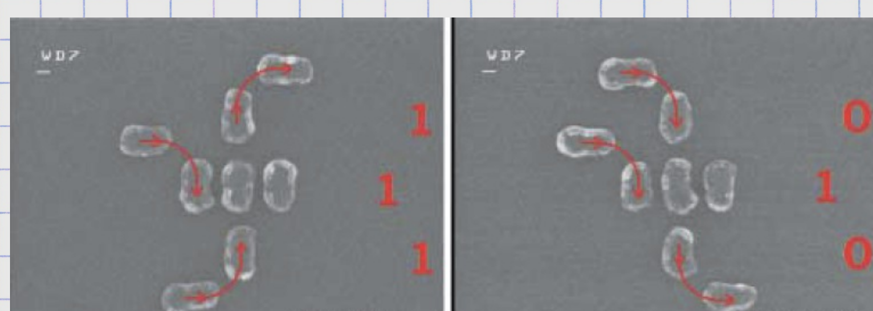

Here : majority gate

A. Imre et al., Science 311, 205 (2006)

Logic (Field driven)

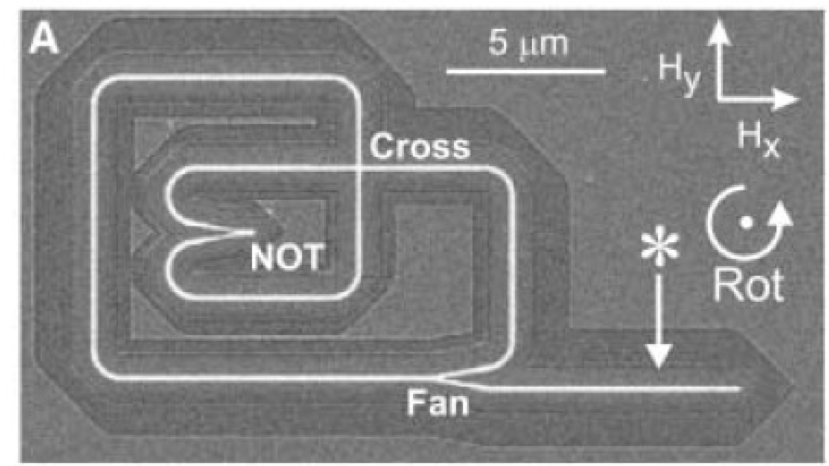

D. A. Allwood et al., Science 309, 1688 (2005)

Memory (current-driven)

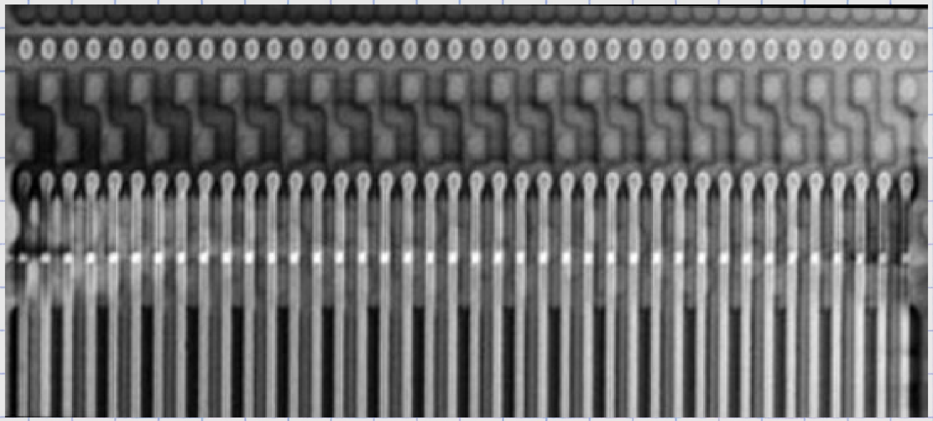

L. Thomas et al., IEEE International Electron Devices meeting (2001)

Towards data 3D storage?

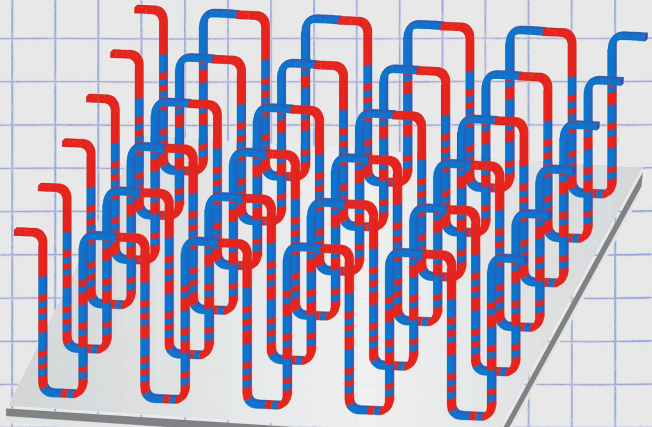

S. S. P. Parkin, Science 320, 190 (2008)
Scientific American 76 (2009) + patents (IBM)

Take-away meessages

- Fundamental science and device prospects
- Field-driven and later spin-torque-driven

Transverse versus vortex wall (simulations)

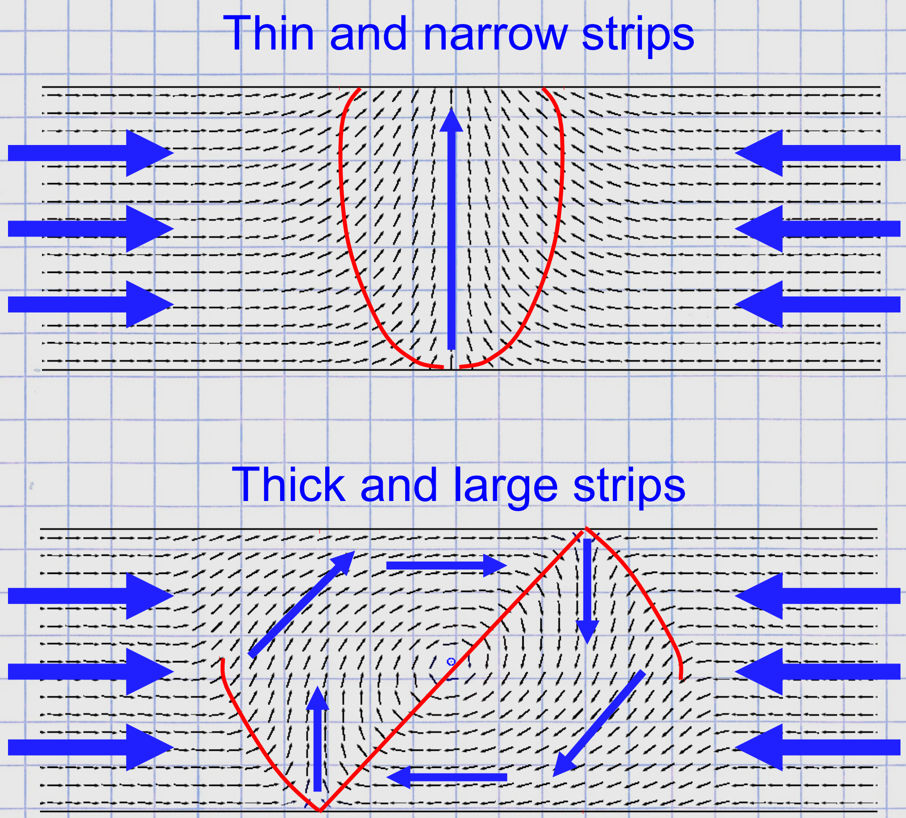

Transition for: $tW \approx 75\,\Delta_{\mathrm{d}}^{2}$

R. McMichael & M. Donahue, IEEE Trans. Mag. 33, 4167 (1997)

Y. Nakatani et al., J. Magn. Magn. Mater. 290-291, 750 (2005)

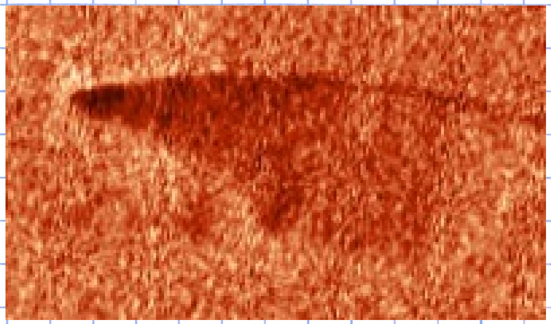

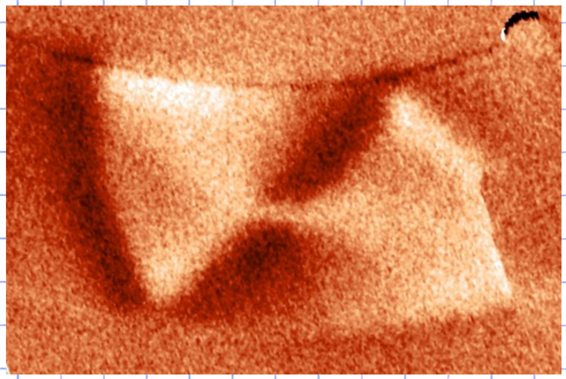

Geometrical pinning

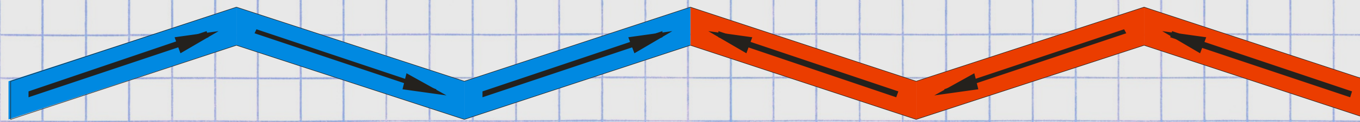

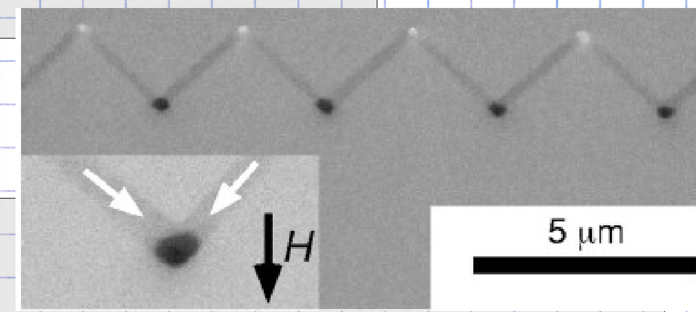

Preparation for in-plane anisotropy

Step 1: transverse field

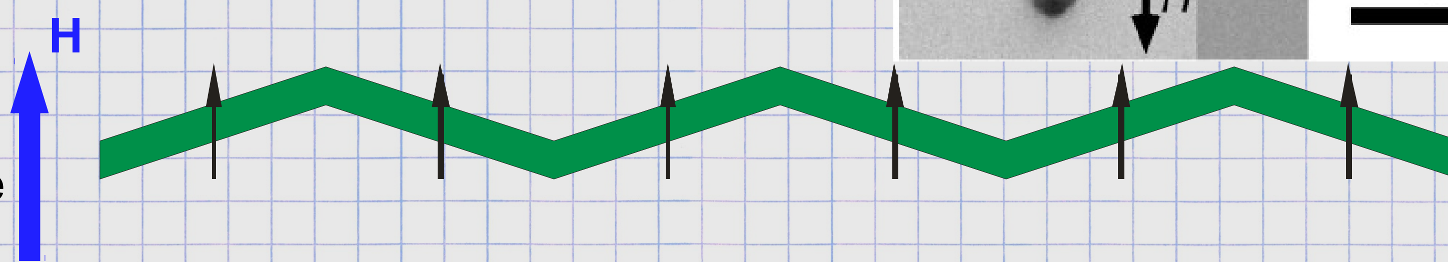

Remanent state

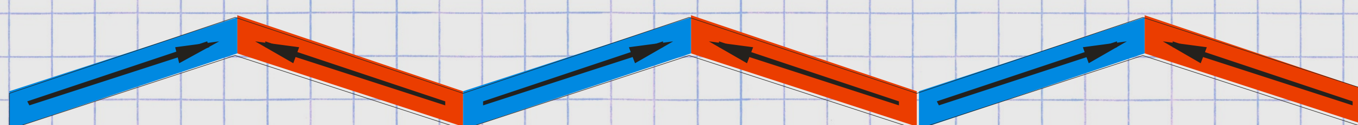

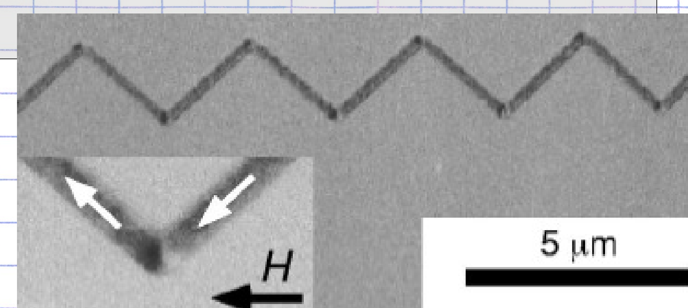

T. Taniyama et al., APL76, 613 (2000)

Disks

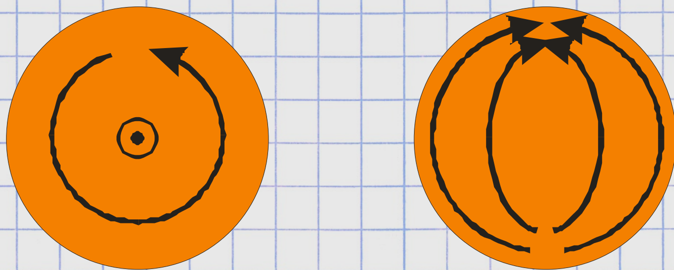

Vortex state

Near single-domain (leaf state)

Aspect ratio D/t

Large diameter D

Rings

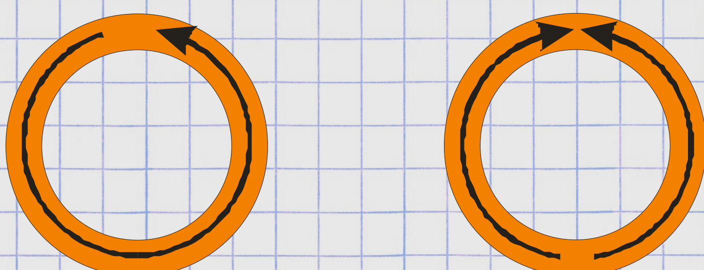

Vortex state

Onion state

Stability less dependent on geometry (no vortex energy)

Control of ring states

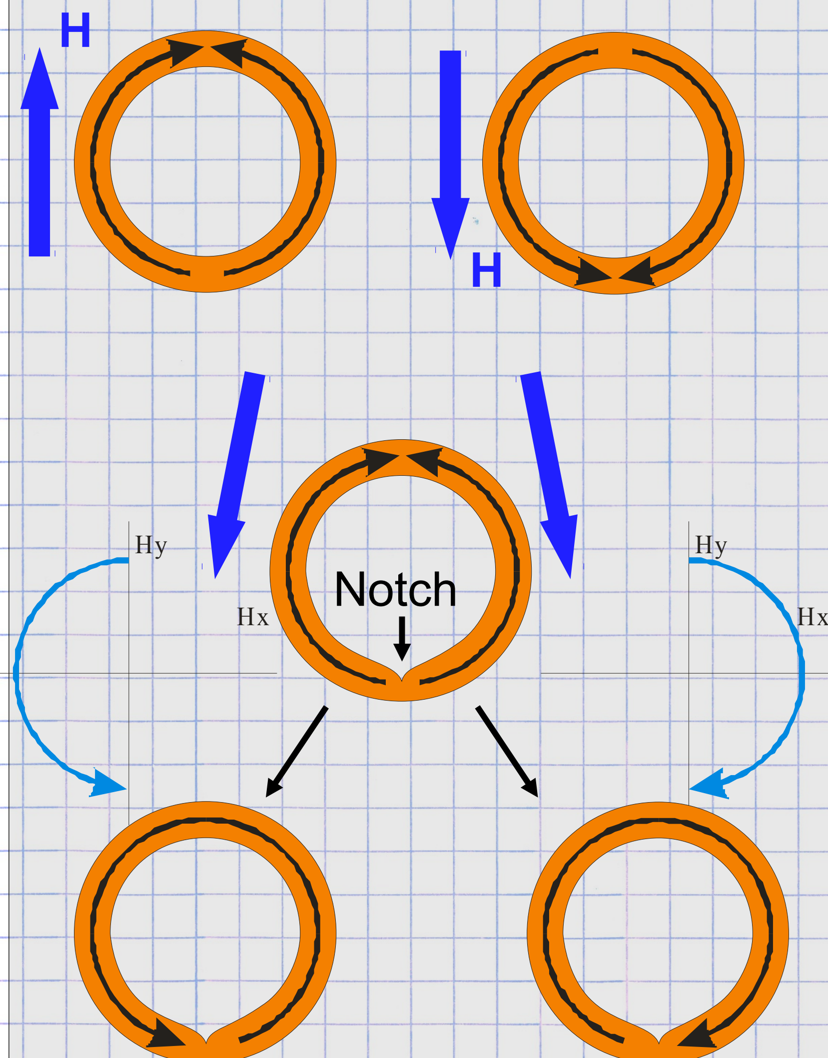

Ex: M. Klaüi et al., APL78, 3268 (2001)

Perpendicular magnetization

Nucleation

Use large pads as domain reservoirs

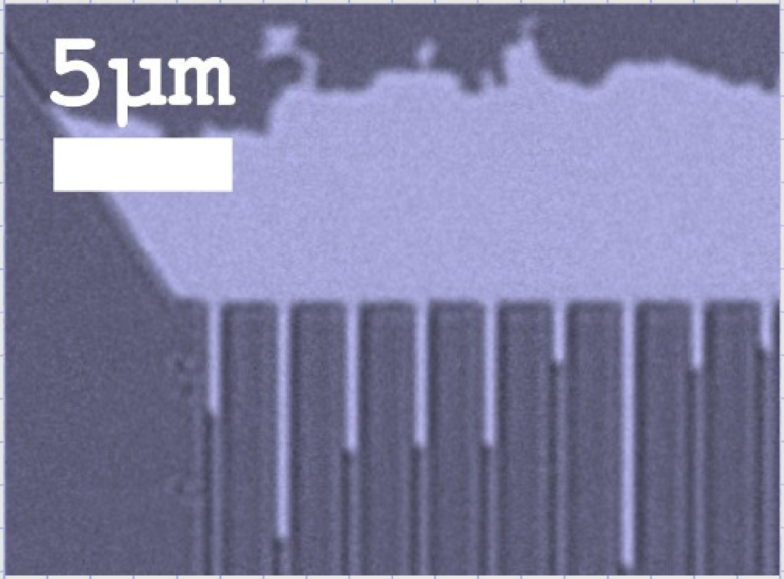

Pt\Co[0.6]\AlOx – Kerr

Courtesy S. Pizzini (NEEL)

Magnetic imaging

Narrow domain walls (2-20nm)

⇨ Shape influenced by disorder

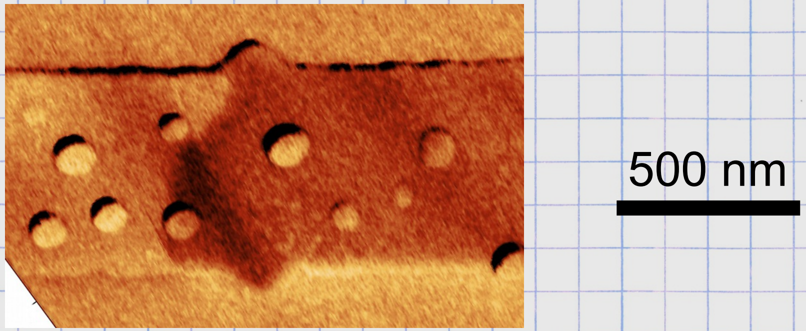

Pt\Co[0.6]\AlOx – MFM

O. Fruchart, unpublished

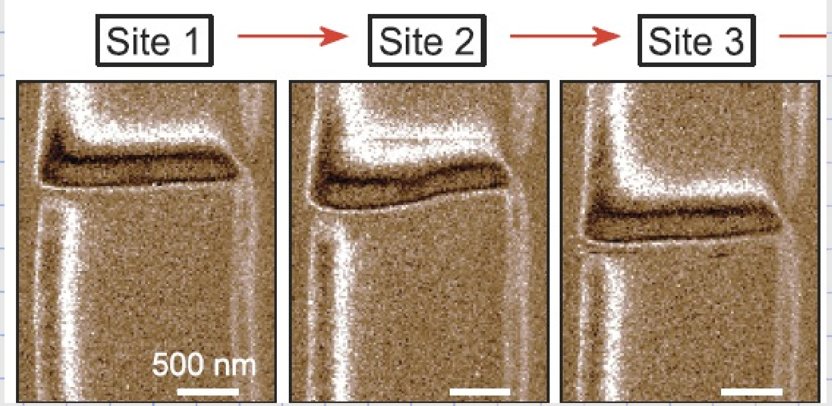

Ta\CoFeB[1]\MgO – NV center

S.P. Tetienne t al., Science 344, 1366 (2014)

Becker-Kondorski model : domain wall to be moved along a 1d landscape

Without applied field

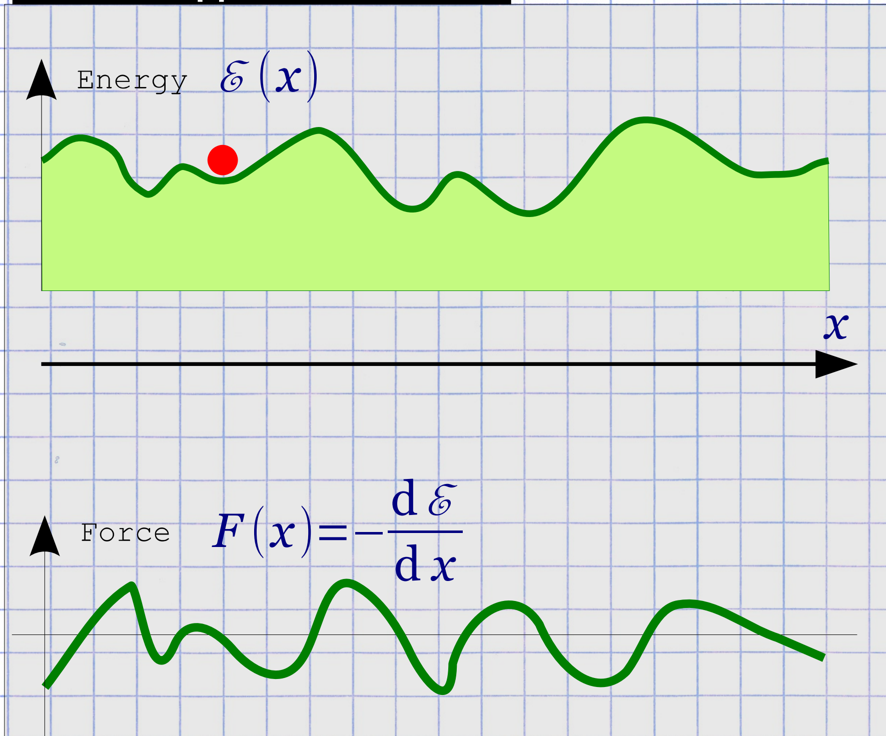

With applied field

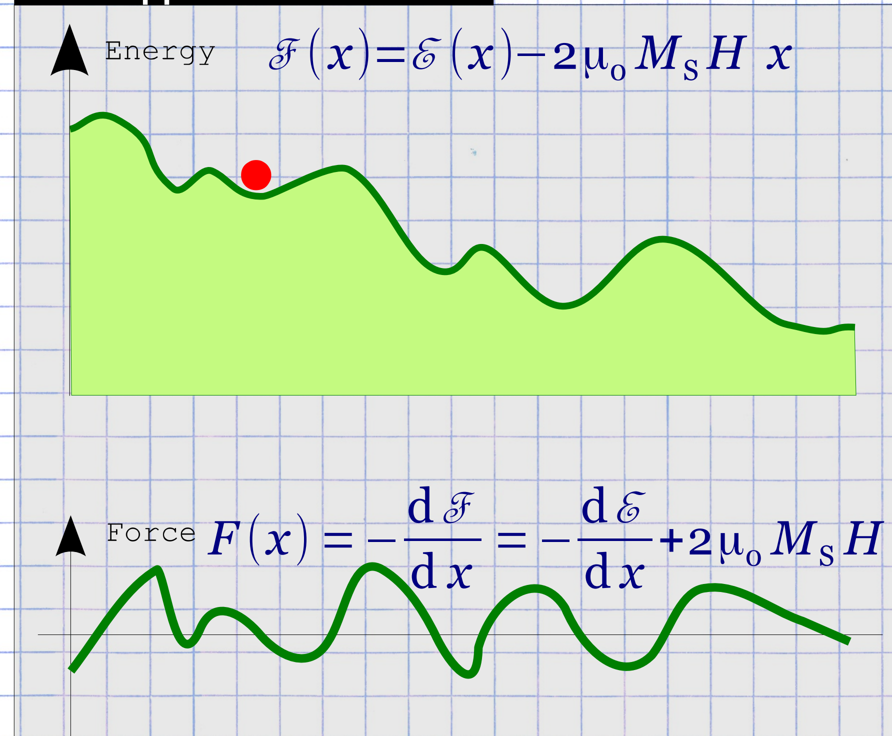

E. Kondorski, On the nature of coercive force and irreversible changes in magnetisation, Phys. Z. Sowjetunion 11, 597 (1937)

Take-away messages

- Propagation field determined by steepest energy gradient
- Microscopic / micromagnetic model needed to build landscape
- Valid only for essentially 1d systems

From 2D to 1D scaling

Creep in strips

Films : $v(H) \sim \exp\left[-\beta U_c \left(\frac{H_{crit}}{H}\right)^{\mu}\right]$ $\mu = 1/4$

⇨ From a rope in 2D to a 1D landscape

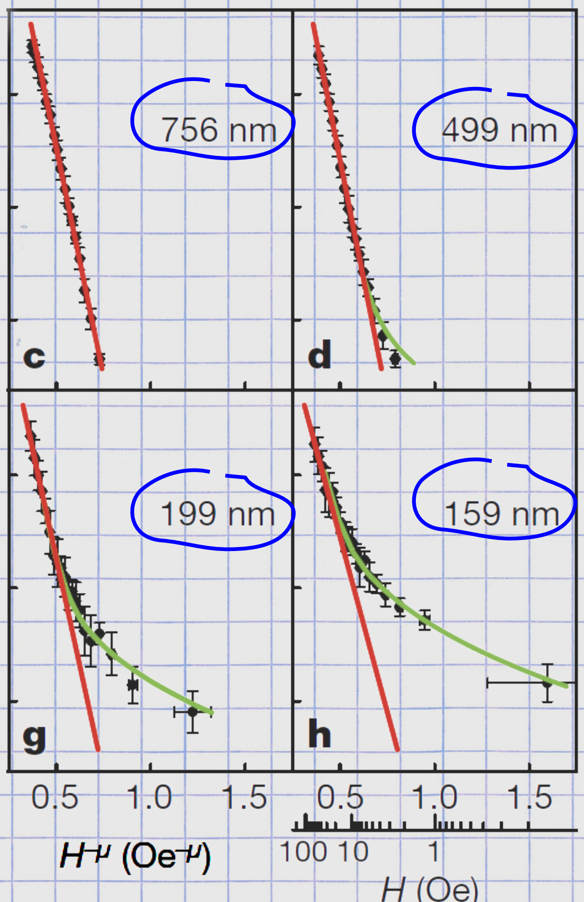

Pt\Co90Fe10[0.3]\Pt
Decreasing strip width

K. J. Kim et al., Nature 458, 740 (2009)

Width-dependent scaling

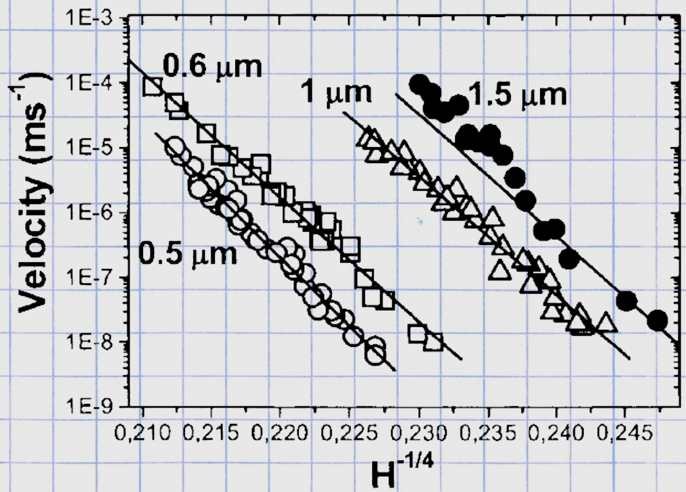

$\mu = 1/4$ ⇨ 2D creep scaling

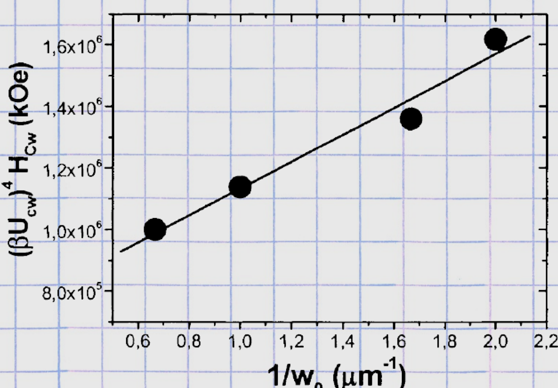

1/w scaling of critical field

⇨ Edge dominated (pseudo-1D)

Pt/Co/Pt film, perpendicular anisotropy

F. Cayssol et al., PRL92 (10, 107202 (2004)

Geometry : 1D

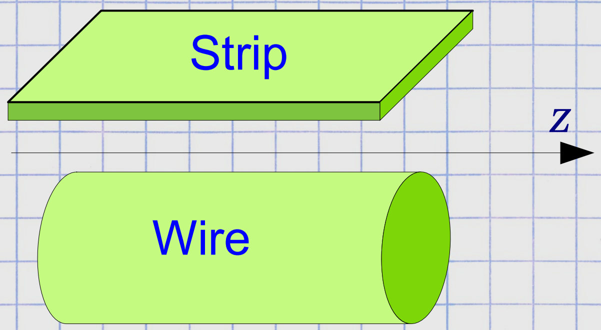

1D model : $\mathbf{m}=\mathbf{m}(z)$

Polar coordinates for magnetization

Azimutal angle

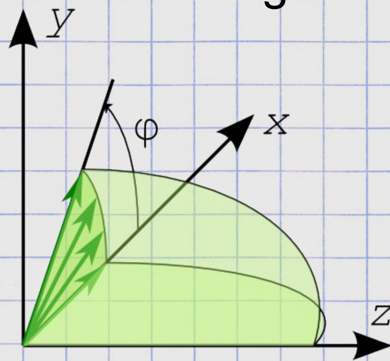

Longitudinal angle

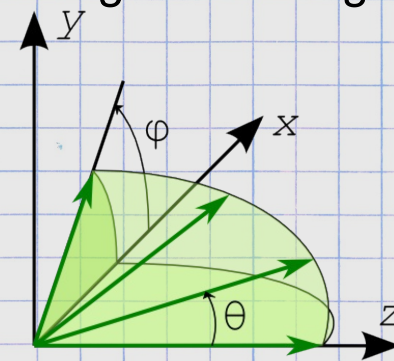

Principle for naïve solving

- Assume uniform azimut : $\left| \begin{array}{l} \varphi=\varphi(t) \\ \theta=\theta(z,t) \end{array} \right.$
- Search for steady-state motion
- Focus on center of domain wall
- Use particulate derivative to convert time variation into motion

$$\frac{\mathrm{D}\mathbf{m}}{\mathrm{D}t}=\frac{\partial \mathbf{m}}{\partial t}+\mathbf{v}.\nabla\mathbf{m}=\mathbf{0} \longrightarrow v=\Delta_{\mathrm{W}}\left(\frac{\mathrm{d}\mathbf{m}}{\mathrm{d}t}.\mathbf{u}_{\theta}\right)$$

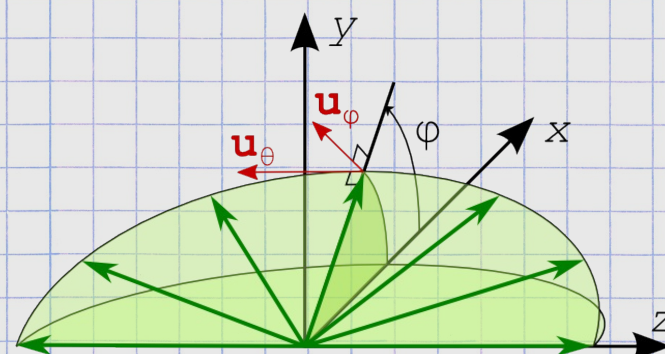

$$\frac{\mathrm{d}\mathbf{m}}{\mathrm{d}t}=-|\gamma_0|\mathbf{m}\times\mathbf{H}+\alpha\,\mathbf{m}\times\frac{\mathrm{d}\mathbf{m}}{\mathrm{d}t}$$

NB : $\gamma_0<0$

Notations

$$\frac{\mathrm{d}\mathbf{m}}{\mathrm{d}t}=-|\gamma_0|\mathbf{m}\times\mathbf{H}+\alpha\,\mathbf{m}\times\frac{\mathrm{d}\mathbf{m}}{\mathrm{d}t}$$

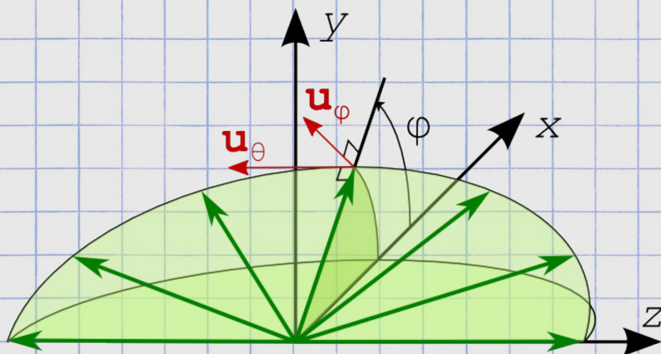

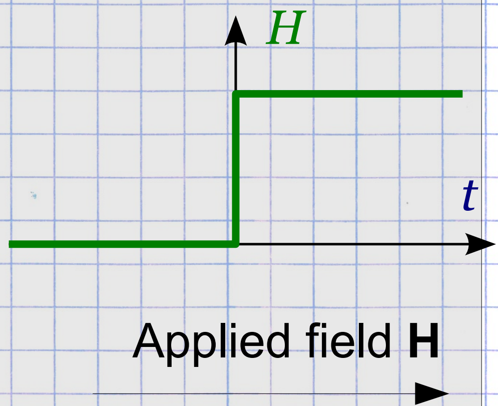

Solving

$$\frac{\mathrm{d}\mathbf{m}}{\mathrm{d}t}=\left.\frac{\mathrm{d}\mathbf{m}}{\mathrm{d}t}\right|_{\mathbf{H}}=-|\gamma_0|\mathbf{m}\times\mathbf{H}=|\gamma_0|H\,\mathbf{u}_\varphi$$

$$\left.\frac{\mathrm{d}\mathbf{m}}{\mathrm{d}t}\right|_{\alpha}=\alpha\,\mathbf{m}\times\left.\frac{\mathrm{d}\mathbf{m}}{\mathrm{d}t}\right|_{\mathbf{H}}=-\alpha|\gamma_0|H\,\mathbf{u}_\theta$$

For $\alpha\ll1$ $\quad \frac{\mathrm{d}\mathbf{m}}{\mathrm{d}t}(t)\approx\left.\frac{\mathrm{d}\mathbf{m}}{\mathrm{d}t}\right|_{\mathbf{H}}=|\gamma_0|H\,\mathbf{u}_\varphi$

Main features

Reminder : $\quad v=\Delta_{\mathrm{W}}\left(\frac{\mathrm{d}\mathbf{m}}{\mathrm{d}t}.\mathbf{u}_\theta\right)$

⇨ Longitudinal speed $\quad v=-\alpha|\gamma_0|H\,\Delta_{\mathrm{W}}$

⇨ Azimutal precession $\quad \omega=|\gamma_0|H$

Fast azimutal precession, slow forward motion

Notations

$$\frac{\mathrm{d}\mathbf{m}}{\mathrm{d}t} = -|\gamma_0|\,\mathbf{m}\times\mathbf{H} + \alpha\,\mathbf{m}\times\frac{\mathrm{d}\mathbf{m}}{\mathrm{d}t}$$

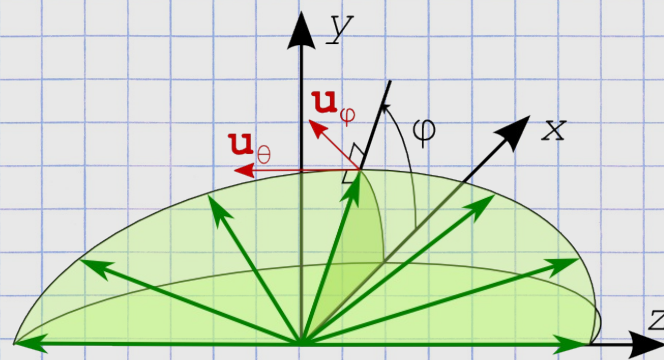

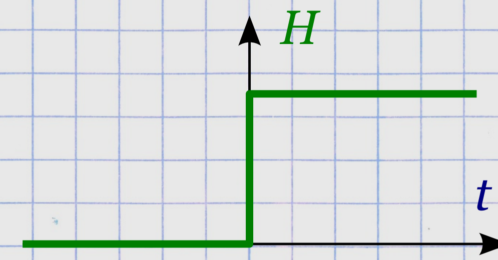

Applied field **H**

Step 1

$$\frac{\mathrm{d}\mathbf{m}}{\mathrm{d}t} = \left.\frac{\mathrm{d}\mathbf{m}}{\mathrm{d}t}\right|_{\mathbf{H}} = -|\gamma_0|\,\mathbf{m}\times\mathbf{H} = |\gamma_0|\,H\,\mathbf{u}_\varphi$$

⇨ Onset of azimutal precession

⇨ Creates demag field $\mathbf{H}_\mathrm{d} = -(\sin\varphi)\,M_\mathrm{s}\,\mathbf{u}_y$

⇨ Similar to precession of a macrospin dot

Later stages

$$\left.\frac{\mathrm{d}\mathbf{m}}{\mathrm{d}t}\right|_{\mathrm{Field}} = \left.\frac{\mathrm{d}\mathbf{m}}{\mathrm{d}t}\right|_{\mathbf{H}} + \left.\frac{\mathrm{d}\mathbf{m}}{\mathrm{d}t}\right|_{\mathbf{H}_\mathrm{d}}$$

$$= \underbrace{|\gamma_0|\,H\,\mathbf{u}_\varphi}_{\text{Precession}} \underbrace{-|\gamma_0|\,M_\mathrm{s}\sin\varphi\cos\varphi\,\mathbf{u}_\theta}_{\text{Forward motion}}$$

$$\left.\frac{\mathrm{d}\mathbf{m}}{\mathrm{d}t}\right|_{\alpha} = \alpha\,\mathbf{m}\times\left.\frac{\mathrm{d}\mathbf{m}}{\mathrm{d}t}\right|_{\mathrm{Field}}$$

$$= \underbrace{-\alpha|\gamma_0|\,H\,\mathbf{u}_\theta}_{\text{Weak forward motion}} \underbrace{-\alpha|\gamma_0|\,M_\mathrm{s}\sin\varphi\cos\varphi\,\mathbf{u}_\varphi}_{\text{Opposes precession}}$$

Balance for $\sin 2\varphi = \dfrac{2H}{\alpha M_\mathrm{s}}$

Define Walker field : $H_\mathrm{W} = \alpha M_\mathrm{s}/2$

N. L. Schryer et al., JAP45, 5406 (1974)

Motion below the Walker field

Steady-state azimut : $\sin 2\varphi = \dfrac{2H}{\alpha M_s}$

High speed $\quad v = |\gamma_0| \Delta_W H/\alpha \sim 1/\alpha$

Δ_W Is a dynamic parameter and is not the DW width at rest

Motion above the Walker field

- Precession with non-steady angular speed
- Soon recovers speed $\quad v \approx \alpha |\gamma_0| H \Delta_W$

$v_W = |\gamma_0| \Delta_W M_s/2$ Walker speed limit

Motion below the Walker field

$v_W = |\gamma_0| \Delta_W M_s/2$

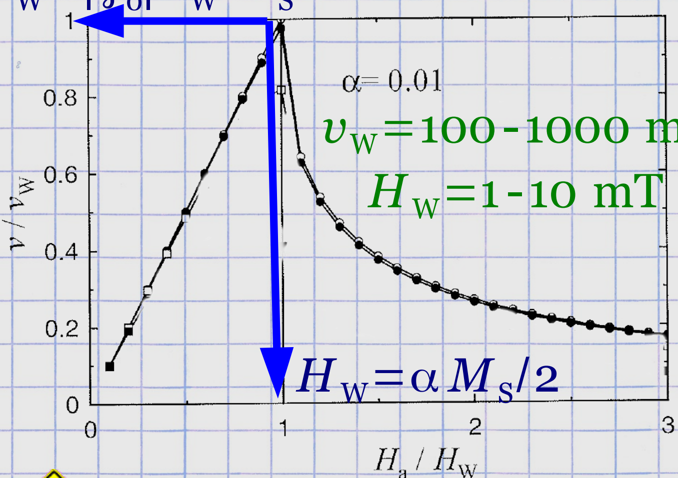

$v_W = 100\text{-}1000$ m/s

$H_W = 1\text{-}10$ mT

$H_W = \alpha M_s/2$

Micromagnetics modify these figures

Experimental confirmation

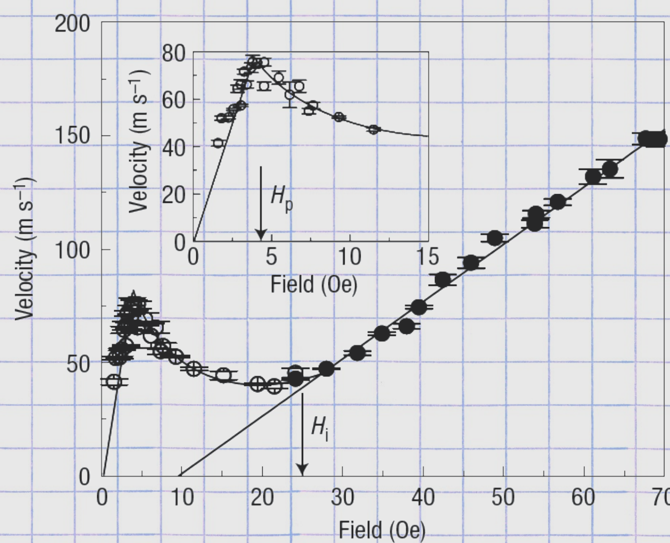

Py(20nm) strips 600nm wide

G. S. D. Beach et al., Nat. Mater. 4, 741 (2005)

A. Thiaville & Y. Nakatani, in Spin dynamics in confined magnetic structures III, B. Hillebrands & A. Thiaville (ed.), Springer, 101, 161-206 (2006)

Closure domains (flat)

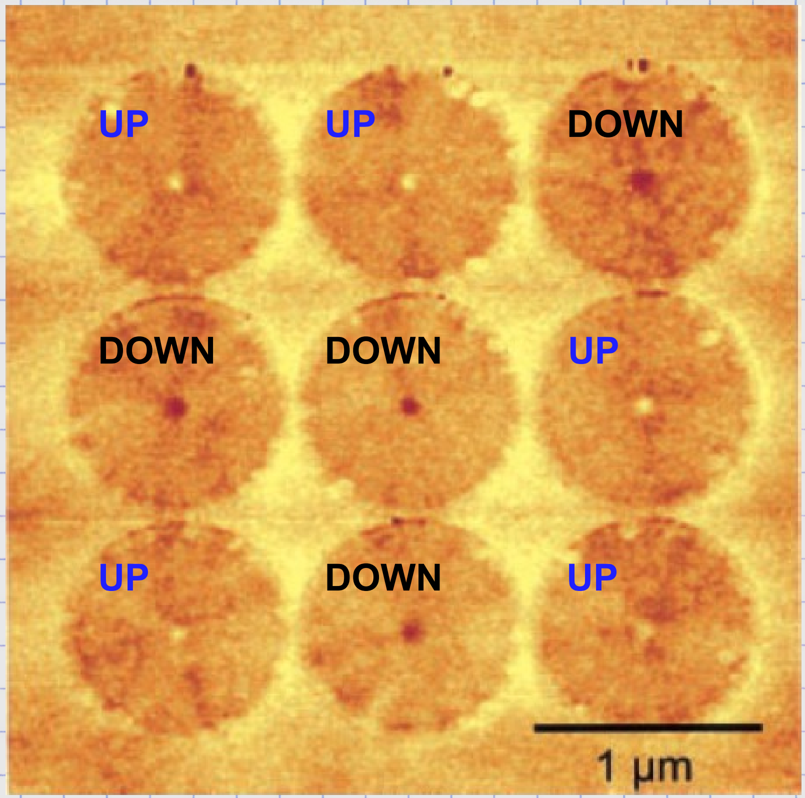

Fig. 2. MFM image of an array of permalloy dots 1 µm in diameter and 50 nm thick.

The central magnetic vortex may be magnetized up or down using a perpendicular field

T. Shinjo et al., Science 289, 930 (2000)
T. Okuno et al., JMMM240, 1 (2002)

Theory and simulation

Simulation

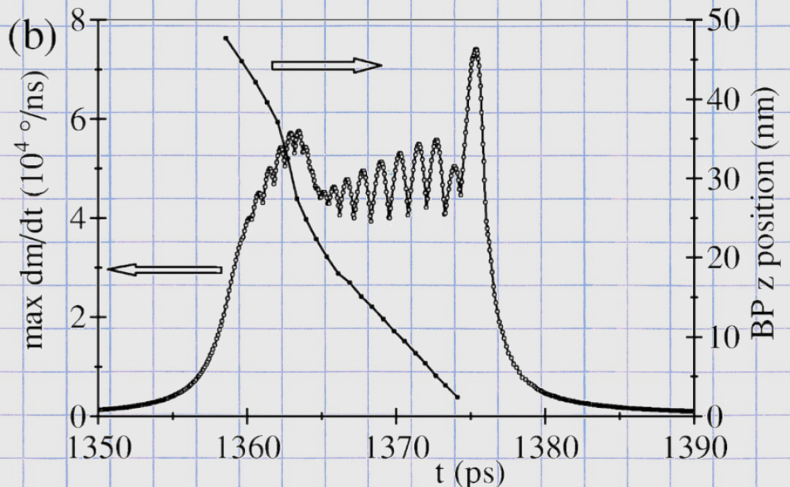

A. Thiaville et al., Phys. Rev. B 67, 094410 (2003)

Requires a Bloch point
→ Not well described in micromagnetism

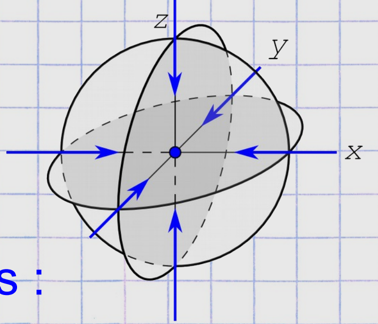

Multiscale simulations :

C. Andreas et al., JMMM 362, 7 (2014)

First theoretical insight in Bloch points :

W. Döring, J. Appl. Phys. 39, 1006 (1968)

Bloch domain wall in the bulk (2D)

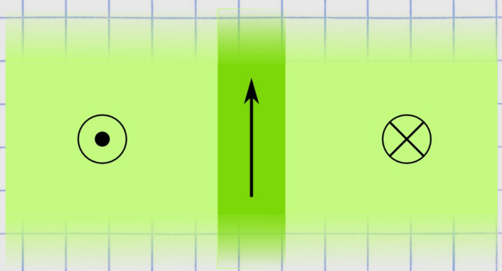

- No magnetostatic energy
- Width $\Delta_u = \sqrt{A/K}$
- Areal energy $\gamma_W = 4\sqrt{AK}$

Other angles & anisotropy

F. Bloch, Z. Phys. 74, 295 (1932)

Domain walls in thin films (2D → 1D)

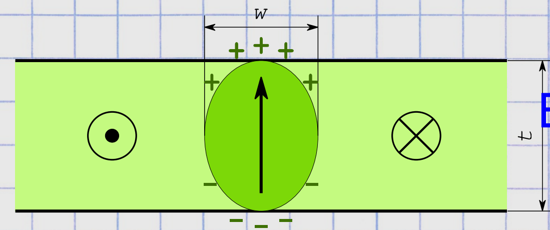

Bloch wall

$t \gtrsim w$

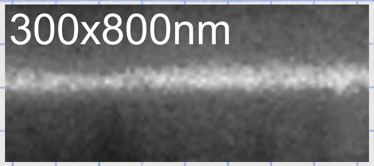

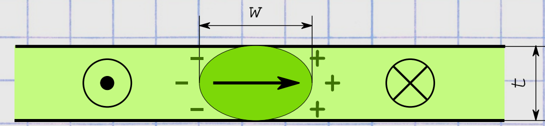

Néel wall

$t \lesssim w$

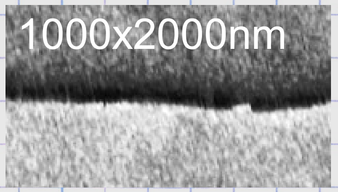

- Contains magnetostatic energy
- No exact analytics

L. Néel, C. R. Acad. Sciences 241, 533 (1956)

Constrained walls (eg : in stripes)

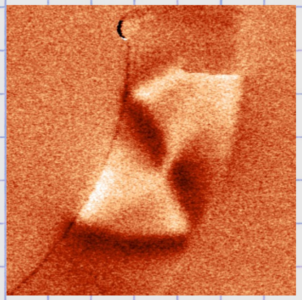

Permalloy (15nm)
Strip 500nm

Magnetic vortex (1D → 0D)

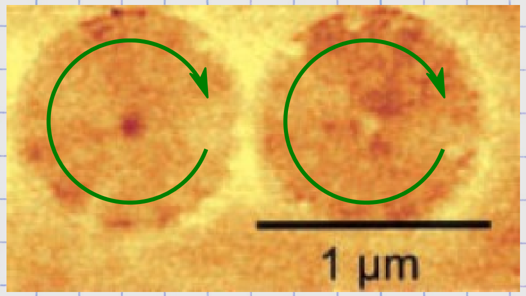

T. Shinjo et al., Science 289, 930 (2000)

Bloch point (0D)

- Point with vanishing magnetization

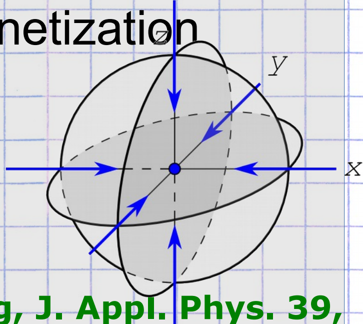

W. Döring, J. Appl. Phys. 39, 1006 (1968)

Exchange interaction (reminder)

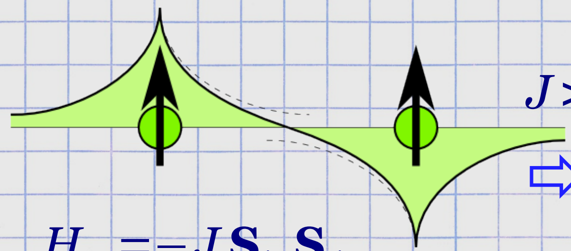

$J>0$

⇨ Ferromagnetic alignment

$$H_{\mathrm{ex}} = -J\,\mathbf{S}_i . \mathbf{S}_j$$

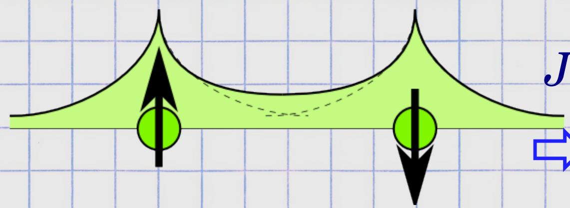

$J>0$

⇨ Antiferromagnetic alignment

Experimental confirmations

Thinned bulk $Fe_{0.5}Co_{0.5}Si$, Lorentz microscopy

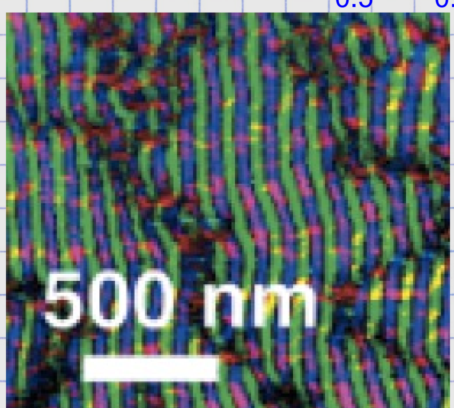

NB : requires low temperature

M. Uchida et al., Science 311, 359 (2006)

Dzyaloshinskii-Moriya Interaction (DMI)

⇨ Favors non-colinear alignment via interaction with non-magnetic atom

⇨ Requires a non-centro symmetric environment for non-cancelation

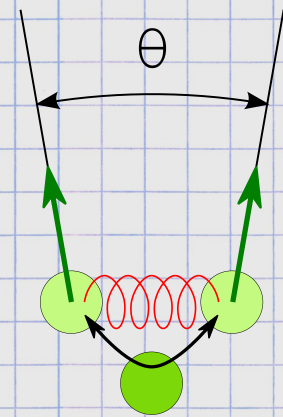

$$H_{\mathrm{ex}} = \mathbf{d}_{ij} . \left(\mathbf{S}_i \times \mathbf{S}_j\right)$$

- Favors spirals or cycloids
- $\mathbf{d}_{ij} = -\mathbf{d}_{ji}$ selects a unique chirality

I. E. Dzyaloshinskii, Sov. Phys. JETP 5, 1259 (1957)

T. Moriya, Phys. Rev. 120, 91 (1960)

Skyrmions under applied field

Thinned $Fe_{0.5}Co_{0.5}Si$, Lorentz microscopy

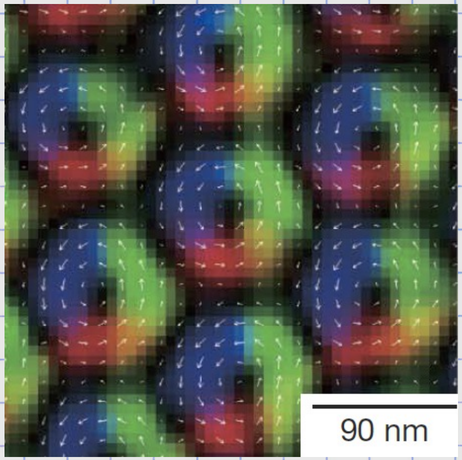

⇨ Arrays only

⇨ Present case : spiral order

X. Z. Yu et al., Nature 465, 901 (2010)

Thin films as artificial materials

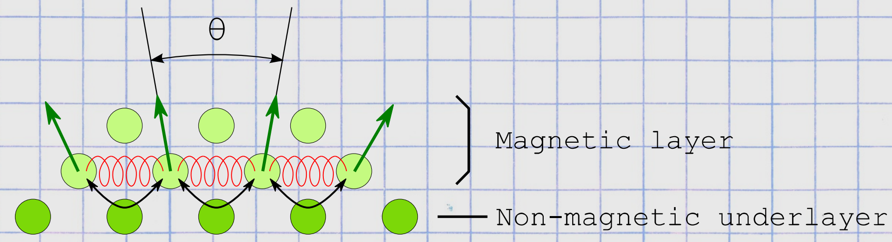

⇨ Should bring more versatility, and operation at room temperature

⇨ $\mathbf{d}_{ij} = d\,\mathbf{u}_{ij} \times \mathbf{n}$ favoring cyloids

⇨ Interfacial effect

Thin film results

Ir(111)\Fe\Pd, sp-STM

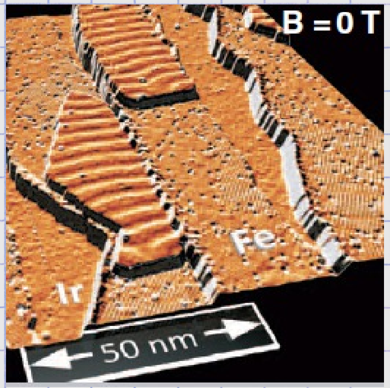

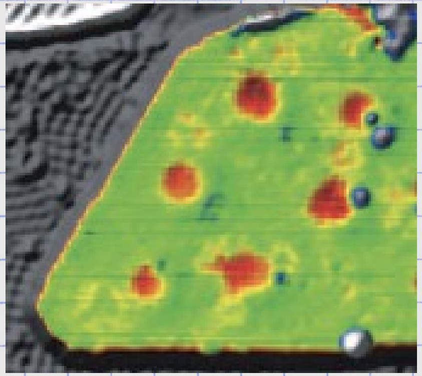

Cycloids

Single skyrmions

N. Romming et al., Science 341, 636 (2013)

Micromagnetics

⇨ Isolated skyrmions as metastable objects, moved with current

S. Rohart et al., PRB 88, 184422 (2013)

A. Fert et al., Nat. Nanotech 8, 152 (2013)